

16 Heavy Flavors

As shown in Fig. 15.15, the energy point $\simeq 1$ GeV separates the QCD scale into regions of large and small running coupling $\alpha_s(\mu)$, or equivalently, of low and high energy, or light and heavy particles. The world of heavy flavors begins with the charm quark and the τ lepton and extends to the bottom and top quarks in the fermionic sector. The list of heavy particles in the standard model also includes the weak bosons W^\pm and Z^0 , and the neutral Higgs boson. Of these, only the Higgs boson is still not experimentally observed at present.

Once a particle is produced, its decay provides the traditional way to determine its intrinsic properties and its characteristic interactions with other particles. Let us recall a few examples: P and CP violations were revealed by K^+ and K^0 decays; the extremely narrow width of the heavy J/ψ signaled its presence; charm was discovered by its typically dominant decay into strangeness; the τ^\pm lepton pair was recognized by the distinctive signature $e^\pm \mu^\mp$ left by its leptonic decays.

For the B meson studied in this chapter, its decays are particularly interesting for the following reasons:

(i) due to the QCD asymptotic freedom and the large masses and momenta released by heavy flavors, electroweak and strong interactions are closely correlated. Their interplay in perturbative calculations can be further improved by the renormalization group methods. The first section is devoted to the QCD renormalization of weak interactions which provides a basis for nonleptonic decays.

(ii) a new symmetry – called heavy flavor symmetry (HFS) – appears in an effective Lagrangian derived from QCD in the limit $M \rightarrow \infty$ (M being the heavy quark mass). This symmetry allows the determination of the form factors involved in the exclusive decay modes. Some of these predictions play a crucial role in determining the CKM matrix elements. The $1/M$ expansion provides a solid theoretical framework for the spectator model in which only the heavy quark undergoes decay while the light constituents are spectators. Semileptonic decays are the best way to understand many properties of the b-flavored hadrons and to measure V_{cb} and V_{ub} .

(iii) the physics of heavy particles has their impact on various quantities through their quantum effects in loops. For instance, from the observed B^0 – \bar{B}^0 mixing, a lower bound of the top mass is predicted before its discovery.

(iv) the physics of heavy flavors plays an essential role in CP violation too, and may open windows on the mechanism of the gauge symmetry breaking, i.e. the Higgs sector.

16.1 QCD Renormalization of Weak Interactions

In (13.1) and (13.2), the effective Lagrangian for nonleptonic (or hadronic) decays of hadrons is given in the most general form by

$$\frac{G_F}{\sqrt{2}} H^\mu H_\mu^\dagger, \quad \text{with } H_\mu = \sum_{Q,q} V_{Qq} H_\mu^{Qq}, \quad H_\mu^{Qq} = \bar{Q} \gamma_\mu (1 - \gamma_5) q. \quad (16.1)$$

This universal effective Lagrangian governs the hadronic decays of all flavored hadrons, from strange to charm and bottom. Unflavored hadrons (like the neutron and the pion) weakly decay only in semileptonic modes by the lack of a sufficiently large phase volume, while the top quark directly decays into the real W boson and the b quark, $t \rightarrow W + b$, without passing by (1). As for the semileptonic decays of hadrons, they are governed by

$$\frac{G_F}{\sqrt{2}} [H^\mu L_\mu^\dagger + L^\mu H_\mu^\dagger], \quad (16.2)$$

where L_μ is the leptonic current given by (13.2).

In weak decays of hadrons, we note the prominent role of the quark current H^μ . Since quarks interact through QCD, the effect of the hard (energetic) gluons on H^μ alone, as well as on the product $H^\mu H_\mu^\dagger$, must be taken into account. This is called the QCD renormalization of weak interactions to which this section is devoted. The reason for considering hard gluons is that they can be treated within the QCD perturbative framework, due to the asymptotic freedom. Nonperturbative soft gluons effects related to form factors will be studied within the framework of HFS in Sect. 3.

Let us start by considering as an example the hadronic decays of the \bar{B} mesons ($b\bar{q}$ bound states) into charmed and unflavored hadrons. These modes are described by the decay $b \rightarrow c + d + \bar{u}$ (Fig. 16.1). This is the spectator model where the b constituent of the \bar{B} undergoes decay while the light \bar{q} constituent is a spectator.

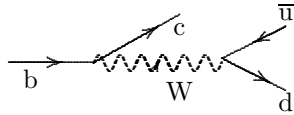


Fig. 16.1. $b \rightarrow c + d + \bar{u}$ at the electroweak tree level

The corresponding effective Lagrangian is the product of the two Cabibbo-favored currents $V_{cb} H_\mu^{bc}$ and $V_{ud}^* H_\mu^{\mu\dagger}$

$$i \left(\frac{-ig}{2\sqrt{2}} \right)^2 V_{cb} V_{ud}^* \frac{-i}{k^2 - M_W^2} (H_\mu^{bc}) (H_\mu^{\mu\dagger}) \xrightarrow{k^2 \ll M_W^2} \frac{G_F}{\sqrt{2}} V_{cb} V_{ud}^* \mathcal{O}_A,$$

$$\text{where } \mathcal{O}_A = (H_\mu^{bc}) (H_\mu^{\mu\dagger}) = [\bar{c} \gamma_\mu (1 - \gamma_5) b] [\bar{d} \gamma^\mu (1 - \gamma_5) u]. \quad (16.3)$$

16.1.1 Corrections to Single Currents

Before considering the gluonic corrections to the product $H^\mu H_\mu^\dagger$ which governs nonleptonic decays, let us discuss the QCD effect on the single currents H^μ ; these corrections concern also the semileptonic modes. In fact, we are already familiar with the latter in Chap. 14 which treats the correction to H_{ud}^μ (we call it from now on the ‘right vertex’ [ud]). The corrections apply to H_{bc}^μ , the ‘left vertex’ [bc] too.

For each of these two vertices ([ud] or [bc]) taken separately, there are in all five Feynman diagrams shown in Fig. 14.2 (virtual gluons) and Fig. 14.3 (real gluons) that contribute to the corrections. They are symbolically represented by a \bullet in Fig. 16.2 for the right vertex and in Fig. 16.3 for the left vertex.

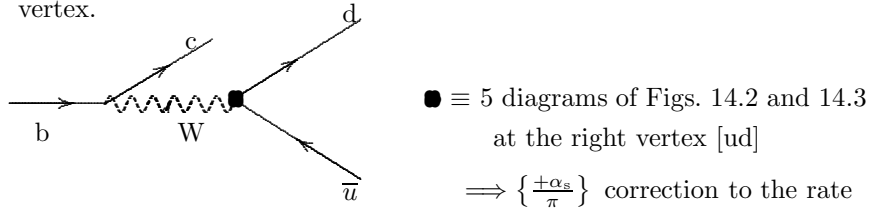


Fig. 16.2. QCD corrections to the right vertex [ud] in $b \rightarrow c + d + \bar{u}$

For the right vertex [ud] part, the one-loop QCD correction to the *rate* of $b \rightarrow c + d + \bar{u}$ is equal to the one found in $\tau^- \rightarrow \nu_\tau + d + \bar{u}$, i.e.

$$N_c \frac{G_F^2 M^5}{192\pi^3} |V_{cb} V_{ud}^*|^2 \left\{ \frac{\alpha_s}{\pi} \right\} \equiv N_c \Gamma_0 |V_{cb} V_{ud}^*|^2 \left\{ \frac{\alpha_s}{\pi} \right\}, \quad (16.4)$$

where $\Gamma_0 = G_F^2 M^5 / (192\pi^3)$ as given by (13.21) is the width of the fermion b of mass M decaying into three massless fermions c , d , and \bar{u} . For massive c , d and \bar{u} quarks, the rate Γ_0 is to be multiplied by the phase space suppression factor $I(x, y, z)$ as given by (13.63). The rate Γ_0 and the coefficient $|V_{cb} V_{ud}^*|^2$ are implicitly understood in the following. The factor α_s/π represents the one-loop QCD correction to the right vertex [ud] (see 14.83).

To convert the $\bar{u}d$ pair into hadrons in the inclusive rate $\tau^- \rightarrow \nu_\tau + \text{hadrons}$ (or $\bar{B} \rightarrow \text{hadrons}$), the color factor $N_c = 3$ must be included in (4) [see also (14.83) and (69) below].

For massive d and \bar{u} quarks associated with this right [ud] vertex, the correction becomes larger than α_s/π [see the function $K(x, y)$ in Table 14.1]. In $b \rightarrow c + d + \bar{u}$, for any fixed value of the c quark mass of the left part, the right vertex correction grows with the increasing masses of its associated u , d quarks and is always positive. This dynamical enhancement is completely different from the purely kinematic phase space suppression effect due to the c quark mass. For instance, in $b \rightarrow c + s + \bar{c}$, the $s\bar{c}$ pair replaces the $d\bar{u}$ pair, the correction to the right vertex [cs] is considerably larger than α_s/π because the s and \bar{c} masses largely exceed the d and \bar{u} masses.

The QCD corrections to the left vertex [bc] shown in Fig. 16.3 can be computed with the five similar diagrams as in Chap. 14. The result

$$-\frac{2}{3} \frac{\alpha_s}{\pi} \left[\pi^2 - \frac{25}{4} \right] = -2.41 \frac{\alpha_s}{\pi} \quad (16.5)$$

is taken from the electromagnetic corrections to $\mu^- \rightarrow \nu_\mu + e^- + \bar{\nu}_e$ already given by (13.27), with the substitution $e^2 \rightarrow \frac{4}{3}g_s^2$.

As noted in Chap. 14, the factors π^2 – coming from the second derivative of the $\Gamma(x)$ function in both real and virtual gluon diagrams – do not exactly cancel each other in this left vertex [bc] (while they do in the right vertex), so we have the π^2 term in (5).

The formula (5) is valid only for massless c, u, and d quarks in the final state. When quarks are massive, the result while remaining negative is reduced in magnitude. For instance, with $m_c = 0.3 M$ and $m_u = m_d = 0$, the QCD correction to the rate is $-0.87 (\alpha_s/\pi)$ instead of $-2.41 (\alpha_s/\pi)$, always with the multiplicative factor $\Gamma_0 |V_{cb} V_{ud}^*|^2$.

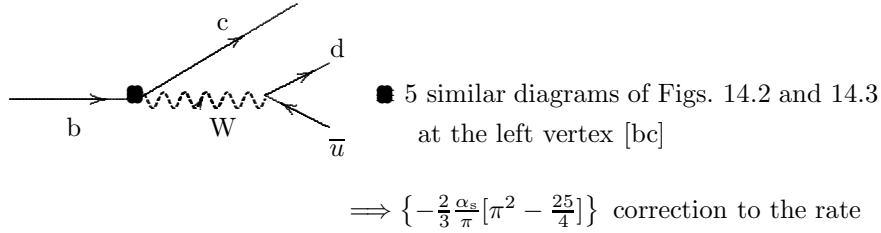


Fig. 16.3. QCD corrections to the left vertex [bc] in $b \rightarrow c + d + \bar{u}$

The overall corrections to nonleptonic decays $b \rightarrow c + d + \bar{u}$ coming from the left and right vertices are (the common factor $N_c \Gamma_0 |V_{cb} V_{ud}^*|^2$ in (4) and (5) is implicit):

$$\frac{-2\alpha_s}{3\pi} \left(\pi^2 - \frac{25}{4} \right) + \frac{\alpha_s}{\pi} = \frac{-2\alpha_s}{3\pi} \left(\pi^2 - \frac{31}{4} \right) = -1.41 \frac{\alpha_s}{\pi} . \quad (16.6)$$

This formula is valid for the three massless quarks in the final state. For $m_c = 0.3 M$ and $m_u = m_d = 0$, the overall corrections are no more (6) but change into $[-0.87 + 0.52](\alpha_s/\pi) = -0.35 (\alpha_s/\pi)$. The $-0.87(\alpha_s/\pi)$ factor comes from corrections to the left vertex [bc] as mentioned above, while the $0.52(\alpha_s/\pi)$ comes from corrections to the right vertex [ud]. The purely kinematic phase space suppression effect of the c quark mass on the correction to the right vertex [ud] is given by $0.52 (\alpha_s/\pi)$, instead of (α_s/π) when c, u, and d quarks are massless.

In the decay $b \rightarrow c + s + \bar{c}$ (Fig. 16.4) responsible for the mode $\bar{B} \rightarrow J/\psi + \bar{K}$ (Fig. 16.9), we note that the quark mass effect in QCD correction

is much more important¹. Instead of the negative value $-1.41(\alpha_s/\pi)$ for the three massless quarks in the final state as given by (6), the mass effect reverses the sign resulting in an overall positive sign $+3.02(\alpha_s/\pi)$. This is because of the massive s and \bar{c} quarks in the right vertex $[cs]$ which replace the d and \bar{u} [again see the function $K(x, y)$]. This $\bar{B} \rightarrow J/\psi + \bar{K}$ mode is particularly important for the study of CP violation in B mesons (Sect. 5).

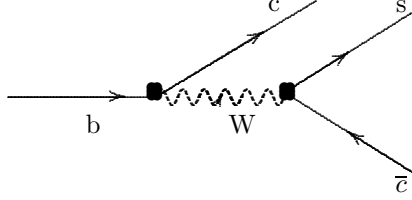


Fig. 16.4. QCD corrections to the left and right vertices in $b \rightarrow c + s + \bar{c}$

These two types of corrections involving the single currents H_μ apply also to the semileptonic modes. For instance, the right vertex $[q_2 q_3]$ correction which occurs in $\tau \rightarrow \nu_\tau + q_2 + \bar{q}_3$ is already studied in Chap. 14. The left vertex $[bc]$ correction, which occurs in the $b \rightarrow c + e^- + \bar{\nu}_e$ decay and describing the inclusive semileptonic decays of B mesons, is given below by (56). They are QCD corrections that have no large logarithmic factors, in contrast to the large logarithmic corrections to the product $H^\mu H_\mu^\dagger$ that we are considering now.

16.1.2 Corrections to Product of Currents

A new type of QCD correction applies to the product $H_\mu^{bc} H_{ud}^{\mu\dagger}$ in which one gluon is exchanged between the two vertices $[bc]$ and $[ud]$ in all possible ways. This correction concerning only hadronic decays has no equivalent in semileptonic modes since gluons are insensitive to leptons. Shown in Fig. 16.5a, the gluon connects the c to the d quark, and in Fig. 16.5b the c to the \bar{u} quark. There are four diagrams in all, the other two are similar (with a gluon exchanged between b and \bar{u} and between b and d) and are not shown.

Our first task is to compute these diagrams. The loop integral with one gluon exchanged between the c and d quarks in Fig. 16.5a yields the term denoted by $I_{c \leftrightarrow d}$, which is given by

$$i \left(\frac{-ig}{2\sqrt{2}} \right)^2 (-ig_s)^2 \int \frac{d^4 k}{(2\pi)^4} \frac{-i}{k^2} \frac{-i}{k^2 - M_W^2} [\bar{d} T^j \gamma^\lambda \frac{i(-\not{k} + m_d)}{k^2 - m_d^2} \gamma^\mu (1 - \gamma_5) u] \\ \times [\bar{c} T^j \gamma_\lambda \frac{i(\not{k} + m_c)}{k^2 - m_c^2} \gamma_\mu (1 - \gamma_5) b], \quad (T^j = \frac{1}{2} \lambda^j). \quad (16.7)$$

¹ Ho-Kim, Q. and Pham, Xuan-Yem, Ann. of Phys. (N.Y.) **155** (1984) 202; Bagan, E., Ball, P., Braun, V. M. and Gosdzinsky, P., Phys. Lett. **342B** (1995) 362; Neubert, M. and Sachrajda, C. T., Nucl. Phys. **B483** (1997) 339.

where the external momenta are taken to be zero but the integration variable k^2 is not neglected (in contrast to (3)). With $m_d \approx 0$, the integral (7) is rewritten as

$$I_{c \leftrightarrow d} = \frac{-i G_F g_s^2}{\sqrt{2}} \int \frac{d^4 k}{(2\pi)^4} \frac{1}{k^2} \frac{M_W^2}{k^2 - M_W^2} \frac{1}{k^2 - m_c^2} \\ \frac{1}{4} \sum_{j=1}^8 [\bar{d}(T^j)_{ef} \gamma^\lambda \gamma^\rho \gamma^\mu (1 - \gamma_5) u] [\bar{c}(T^j)_{gh} \gamma_\lambda \gamma_\rho \gamma_\mu (1 - \gamma_5) b], \quad (16.8)$$

where the color indices e, f, g, h run from 1 to 3, and $1/4$ comes from $k_\sigma k_\rho \rightarrow (1/4)k^2 g_{\sigma\rho}$ (while the summation over the SU(3) index $j = 1, \dots, 8$ in matrix $T^j = \lambda^j/2$ is understood). Writing the product of the three propagators in (8) as an integral over the Feynman auxiliary variables x, y , and applying formulas in the Appendix, we obtain

$$\int \frac{d^4 k}{(2\pi)^4} \frac{1}{k^2} \frac{M_W^2}{k^2 - M_W^2} \frac{1}{k^2 - m_c^2} = \frac{-i}{16\pi^2} \log \frac{M_W^2}{m_c^2} \quad (16.9)$$

after integration first over $\int d^4 k$, then over y and x . This result uses (7) in which the external momenta are neglected. If these momenta are not neglected, the correct lower limit of the logarithm in (9) actually must be set equal to the external momenta which is dominated by the decaying b quark, i.e. $\log(M_W^2/m_c^2)$ should be replaced by $\log(M_W^2/M^2)$.

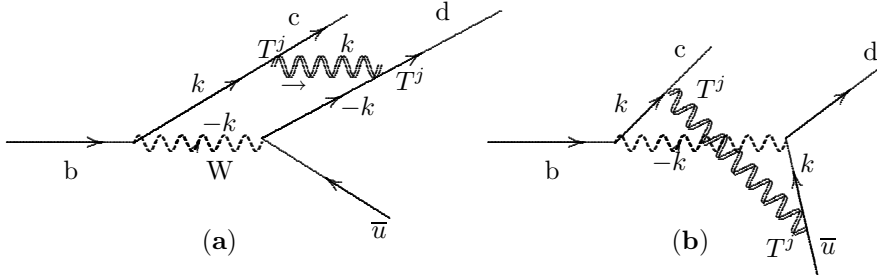


Fig. 16.5a, b. QCD corrections to nonleptonic decays through the product $H^\mu H_\mu^\dagger$. There are two more graphs with a gluon between b and \bar{u} , and between b and d .

This lower limit fixed by the mass M of the decaying particle is easy to understand from the diagram with one gluon exchanged between the b and d (or \bar{u}) quarks, i.e. in (8), we replace m_c by M in their respective propagators.

Let us consider now the second line of (8), which is

$$\{XY\} \equiv \frac{1}{4} \sum_{j=1}^8 [\bar{d} T^j \gamma^\lambda \gamma^\rho \gamma^\mu (1 - \gamma_5) u] [\bar{c} T^j \gamma_\lambda \gamma_\rho \gamma_\mu (1 - \gamma_5) b].$$

We have already met this product without the color matrix T^j in (11.21) and (11.24). Due to (11.23), we have

$$[\bar{d} \gamma^\lambda \gamma^\rho \gamma^\mu (1 - \gamma_5) u] [\bar{c} \gamma_\lambda \gamma_\rho \gamma_\mu (1 - \gamma_5) b] = 16 \mathcal{O}_A, \quad (16.10)$$

where \mathcal{O}_A is given in (3). However, QCD, via the color matrix T^j , drastically changes the dynamics. To simplify notations, let $[\bar{d}(T^j) \gamma^\lambda \gamma^\rho \gamma^\mu (1 - \gamma_5) u]$ stand for $[\bar{d}(T^j) u]$ without the Dirac matrices. Similarly the second factor in (8) is written as $[\bar{c}(T^j) b]$. Then from (11.88) we have

$$\sum_{j=1}^8 [\bar{d}_e T_{ef}^j u_f] [\bar{c}_g T_{gh}^j b_h] = \frac{1}{2} [\bar{d}_e u_f] [\bar{c}_f b_e] - \frac{1}{6} [\bar{d}_e u_e] [\bar{c}_g b_g]. \quad (16.11)$$

Now we reintroduce the Dirac matrices $\gamma^\lambda \gamma^\rho \gamma^\mu (1 - \gamma_5)$ and $\gamma_\lambda \gamma_\rho \gamma_\mu (1 - \gamma_5)$ into the right-hand side of (11), and using again (11.23), we gain a factor of 16 as in the right-hand side of (10). The final result is

$$\begin{aligned} \frac{1}{4} \{XY\} &= \frac{1}{2} [\bar{d}_e \gamma^\mu (1 - \gamma_5) u_f] [\bar{c}_f \gamma_\mu (1 - \gamma_5) b_e] \\ &\quad - \frac{1}{6} [\bar{d}_e \gamma^\mu (1 - \gamma_5) u_e] [\bar{c}_g \gamma_\mu (1 - \gamma_5) b_g]. \end{aligned} \quad (16.12)$$

The second line of the above equation is the product of two color-singlet quark currents, and is nothing but the operator $-\frac{1}{6} \mathcal{O}_A$ in (3). The first line is the product of two color-non-singlet quark currents having the familiar structure $(V - A) \times (V - A)$. This naturally suggests the use of the Fierz transformation which let the structure $(V - A) \times (V - A)$ stay intact (see Appendix). The minus sign from the Fierz rearrangement, when combined with the minus sign from interchanging the order of the anticommuting quark fields, yields an overall positive sign in

$$[\bar{d}_e \gamma^\mu (1 - \gamma_5) u_f] [\bar{c}_f \gamma_\mu (1 - \gamma_5) b_e] = [\bar{d}_e \gamma^\mu (1 - \gamma_5) b_e] [\bar{c}_f \gamma_\mu (1 - \gamma_5) u_f].$$

The right-hand side of the above equation is a product of two color-singlet currents. It is symbolically written as $(\bar{d}b)(\bar{c}u)$ and replaces now the first line of (12). Hence the quantity $\{XY\}$ can also be expressed in terms of two operators, each being the product of *bilinear color-singlet* quark currents: the original one $\mathcal{O}_A \sim (\bar{d}u)(\bar{c}b)$ in (3) and a new operator $\mathcal{O}_B \sim (\bar{d}b)(\bar{c}u)$ emerging from QCD corrections. We have

$$\{XY\} = 2 \mathcal{O}_B - \frac{2}{3} \mathcal{O}_A, \text{ with } \mathcal{O}_B = [\bar{d} \gamma^\mu (1 - \gamma_5) b] [\bar{c} \gamma_\mu (1 - \gamma_5) u]. \quad (16.13)$$

The two color-singlet currents $(\bar{d}b)$ and $(\bar{c}u)$ in \mathcal{O}_B should not be confused with the flavor-changing neutral currents (FCNC) $d \leftrightarrow b$ and $c \leftrightarrow u$ which

never exist because of the GIM mechanism. These apparent FCNC forms arise simply from the Fierz rearrangement. Putting together (8), (9), and (13), we get the contribution of the diagram in Fig. 16.5a:

$$I_{c \leftrightarrow d} = \frac{G_F}{\sqrt{2}} \left\{ \frac{\alpha_s}{4\pi} \log \frac{M_W^2}{M^2} \right\} \left[\frac{2}{3} \mathcal{O}_A - 2 \mathcal{O}_B \right] . \quad (16.14)$$

The contribution $I_{c \leftrightarrow \bar{u}}$ from the diagram in Fig. 16.5b (with the gluon exchanged between the c and \bar{u} quarks) is similarly calculated. Compared with $I_{c \leftrightarrow d}$ in (7), there are two modifications, as seen below:

$$\begin{aligned} i \left(\frac{-ig}{2\sqrt{2}} \right)^2 (-ig_s)^2 \int \frac{d^4 k}{(2\pi)^4} \frac{-i}{k^2} \frac{-i}{k^2 - M_W^2} \left[\bar{d} \gamma^\mu (1 - \gamma_5) \frac{i(+\not{k} + m_u)}{k^2 - m_u^2} \gamma^\lambda T^j u \right] \\ \times \left[\bar{c} T^j \gamma_\lambda \frac{i(\not{k} + m_c)}{k^2 - m_c^2} \gamma_\mu (1 - \gamma_5) b \right] . \end{aligned} \quad (16.15)$$

With the outgoing \bar{u} replacing the outgoing d quark, from (7) to (15) we note an interchange ($+\not{k} \leftrightarrow -\not{k}$) in their propagators. So we obtain

$$[\bar{d} \gamma^\mu (1 - \gamma_5) \gamma^\rho \gamma^\lambda u] [\bar{c} \gamma_\lambda \gamma_\rho \gamma_\mu (1 - \gamma_5) b] = 4 \mathcal{O}_A .$$

The result is $I_{c \leftrightarrow \bar{u}} = -\frac{1}{4} I_{c \leftrightarrow d}$, thus

$$I_{c \leftrightarrow d} + I_{c \leftrightarrow \bar{u}} = \frac{3}{4} I_{c \leftrightarrow d} = \frac{G_F}{\sqrt{2}} \left\{ \frac{\alpha_s}{4\pi} \log \frac{M_W^2}{M^2} \right\} \left[\frac{1}{2} \mathcal{O}_A - \frac{3}{2} \mathcal{O}_B \right] . \quad (16.16)$$

The two remaining contributions $I_{b \leftrightarrow \bar{u}}$ and $I_{b \leftrightarrow d}$ are computed exactly as in (7) and (15). They are respectively equal to $I_{c \leftrightarrow d}$ and $I_{c \leftrightarrow \bar{u}}$, such that the total contributions (from gluon exchanged in all possible ways between the left $[bc]$ and right $[ud]$ vertices) are doubled. Thus

Bare Electroweak	\implies	Renormalization by QCD	
$\frac{G_F}{\sqrt{2}} \mathcal{O}_A$		$\frac{G_F}{\sqrt{2}} \left\{ \frac{\alpha_s}{4\pi} \log \frac{M_W^2}{M^2} \right\} [\mathcal{O}_A - 3 \mathcal{O}_B]$	(16.17)

Compared with the QCD uncorrected (3), the effective operators for nonleptonic decays are modified as follows:

$$\begin{aligned} \mathcal{O}_A &\implies c_A \mathcal{O}_A = \left(1 + \frac{\alpha_s}{4\pi} \log \frac{M_W^2}{M^2} \right) \mathcal{O}_A , \\ 0 &\implies c_B \mathcal{O}_B = -3 \left(\frac{\alpha_s}{4\pi} \log \frac{M_W^2}{M^2} \right) \mathcal{O}_B . \end{aligned} \quad (16.18)$$

The detailed calculation is illustrative. Not only does QCD renormalize the original operator \mathcal{O}_A , it also brings in a new operator \mathcal{O}_B . The operator \mathcal{O}_B ,

which is absent when QCD is neglected, now emerges when gluons enter. Starting from zero, we get $-3[\alpha_s/4\pi](\log M_W^2/M^2)\mathcal{O}_B$.

Furthermore, there is a *logarithmic enhancement* $\log(M_W^2/M^2)$ in the corrections to the product $H^\mu H_\mu^\dagger$ not found in the corrections (4) and (5) to the current H^μ itself. (Hence the adjective ‘leading’ to contrast with nonleading corrections.) This leading logarithmic enhancement concerns only the product $H^\mu H_\mu^\dagger$, i.e. only nonleptonic weak decays. The reason for this enhancement when the gluon in Fig. 16.5 is parallel to or crosses the weak gauge boson W is simple. The logarithmic ultraviolet divergence in the vertex corrections to the single current H^μ is canceled by the same type of divergence as in the quark self-energy (Chap. 14). Whereas for the product $H^\mu H_\mu^\dagger$, the loop integrals of the diagrams in Fig. 16.5 are convergent, we do not need counterterms here, and so the logarithmic enhancement is not removed.

The method just obtained for the $b \rightarrow c + d + \bar{u}$ can be immediately extended to the nonleptonic decays of all other flavored hadrons described by $Q \rightarrow q_1 + q_2 + \bar{q}_3$, for instance $s \rightarrow u + d + \bar{u}$ and $c \rightarrow s + u + \bar{d}$. The only change is in the lower limit (collectively denoted now by μ) of the logarithm $\log(M_W^2/\mu^2)$ in (17). Since the upper limit is always the W mass, the mass scale μ for the lower limit is naturally set equal to the mass of the decaying particles, such that the scale μ is m_s (m_c) for strange (charm) decaying quarks. The logarithmic enhancement is more pronounced in strange than in charm (and *a fortiori* in bottom) nonleptonic decays.

Once we get the effective hadronic weak Lagrangian $H^\mu H_\mu^\dagger$ renormalized by perturbative QCD, we can examine the correction to the decay rate. In Chap. 14, we remark that because of the interference – between the weak-interaction tree amplitude of Fig. 16.1 and the QCD correction to the current H^μ (Figs. 16.2–3) – we get the $\mathcal{O}(\alpha_s)$ correction to the rate as given by (4) and (5). This interference no longer applies to the product $H^\mu H_\mu^\dagger$. Since the color matrix T^j in the diagram of Fig. 16.5 is traceless, the interference between the latter diagram and the tree diagram in Fig. 16.1 vanishes, so we have to square the amplitude of (17) and get $\mathcal{O}(\alpha_s^2)$ corrections to the rate. For the product $H^\mu H_\mu^\dagger$ we gain a logarithmic enhancement but we have a smaller α_s^2 factor in the corrected rate.

16.1.3 Renormalization Group Improvement

In (17), the logarithmic enhancement $\log(M_W^2/m_Q^2)$ for the decaying Q quark is about 6 for bottom ($Q=b$) and 10 for strange ($Q=s$) particles. The perturbative correction to the *decay amplitude* is $\sim \alpha_s \log(M_W^2/m_Q^2)$, of order 1, and so higher-order corrections $[\alpha_s \log(M_W^2/m_Q^2)]^n$ cannot be ignored. These α_s^n corrections correspond to multiple hard gluons exchanged between the two vertices. The renormalization group method discussed in Chap. 15 and illustrated by Fig. 15.10 is particularly adapted to the situation. While it is an impossible task to compute all individual Feynman diagrams, the renormalization group equation can produce the sum of the leading logarithmic terms

to all orders of α_s . Let us rewrite the QCD effects on \mathcal{O}_A taken from (17):

$$\mathcal{O}_A \Rightarrow \mathcal{O}_A + \left\{ \frac{\alpha_s}{2\pi} \log \left(\frac{M_W}{\mu} \right) \right\} [\mathcal{O}_A - 3 \mathcal{O}_B] , \quad (16.19)$$

and note that there is always a mixing between the two operators \mathcal{O}_A and \mathcal{O}_B . The gluonic corrections to \mathcal{O}_B yield a similar result:

$$\mathcal{O}_B \Rightarrow \mathcal{O}_B + \left\{ \frac{\alpha_s}{2\pi} \log \left(\frac{M_W}{\mu} \right) \right\} [\mathcal{O}_B - 3 \mathcal{O}_A] . \quad (16.20)$$

Local operators appear often in quantum loop calculations (see Chap. 11 for box and penguin diagrams), and if they have the same dimension (as in the case of \mathcal{O}_A and \mathcal{O}_B with the dimension six), they are usually mixed. We would like to find combinations of operators that are unmixed by QCD. From (19) and (20), we remark that the operators

$$\mathcal{O}_\pm = \frac{1}{2} [\mathcal{O}_A \pm \mathcal{O}_B] \quad (16.21)$$

satisfy this requirement. They are form-invariant, i.e. unmixed. Using (19) and (20), we note that the bare \mathcal{O}_\pm are *multiplicatively renormalized* by QCD with the coefficient c_\pm :

$$\mathcal{O}_\pm \Rightarrow c_\pm \mathcal{O}_\pm , \quad \text{where } c_\pm = 1 + d_\pm \left[\frac{\alpha_s}{\pi} \log \left(\frac{M_W}{\mu} \right) \right] , \quad (16.22)$$

with $d_+ = -1$ and $d_- = +2$. Then the right hand side of (19) becomes $\mathcal{O}_{NL} = c_+ \mathcal{O}_+ + c_- \mathcal{O}_-$.

We can go farther by summing up all $[\alpha_s \log(M_W/\mu)]^n$ terms with the renormalization group equation. Like the bare and renormalized Green's functions, the operators in field theories can be defined as bare and renormalized operators through their matrix elements. Green's function associated with the operator \mathcal{O}_\pm can be constructed from the four quark fields participating in the decay of $Q \rightarrow q_1 + q_2 + \bar{q}_3$. It is defined as

$$\langle 0 | \mathcal{O}_\pm q_1 q_2 q_3 Q | 0 \rangle , \quad (16.23)$$

where the creation and destruction operators of the quark fields applied to the vacuum $\langle 0 |$ and $| 0 \rangle$ yield the matrix element of \mathcal{O}_\pm . Therefore, through their associated Green's functions, the renormalized operators also obey the Callan–Symanzik (CS) equation, which states that a change in the scale μ must be compensated by their anomalous dimensions through the running coupling constant $\alpha_s(\mu)$, leaving the bare operators independent of μ . We may define the corresponding rescaling factor $Z_{\mathcal{O}}(\mu)$ of any operator \mathcal{O} similarly to the field-strength renormalization functions $Z(\mu)$ which we are familiar with in Chap. 15. Let us define

$$\mathcal{O}^{\text{bare}} = Z_{\mathcal{O}}(\mu) \mathcal{O}^{\text{ren}} .$$

For the problem on hand, the calculation of $Z_{\mathcal{O}_{\pm}}(\mu)$ is already performed. To see how $Z_{\mathcal{O}_{\pm}}(\mu)$ is calculated, let us return again to the logarithm in (19) and note that at the scale $\mu = M_W$, QCD does not bring in any correction to the weak-interaction operators from which we start. The cutoff Λ [or $\Gamma(2 - \frac{n}{2})$] in the regularization of loop integrals is naturally replaced with M_W in the case considered here. It can also be seen by putting $M_W \rightarrow \infty$ in (9), which becomes

$$-\int \frac{d^4 k}{(2\pi)^4} \frac{1}{k^2} \frac{1}{k^2 - m_c^2} = \frac{-i}{16\pi^2} \frac{\Gamma(2 - \frac{n}{2})}{\mu^{4-n}},$$

using the familiar dimensional regularization method. Comparing the above equation with (9), we note that $\log(M_W^2/\mu^2)$ is replaced with $\Gamma(2 - \frac{n}{2})/\mu^{4-n}$.

From the high mass cutoff M_W going down to the scale $\mu = m_Q$ of the decay process $Q \rightarrow q_1 + q_2 + \bar{q}_3$, the bare operators \mathcal{O}_{\pm} are multiplicatively renormalized by c_{\pm} according to (22). So the corresponding $Z_{\mathcal{O}_{\pm}}(\mu)$ are nothing but $c_{\pm}(\mu)$. According to (15.44), the anomalous dimensions $\gamma_{\pm}(g_s)$ which govern the evolution of the operators $\mathcal{O}_{\pm}(\mu)$ can be obtained by taking the derivative of the function $\log Z_{\mathcal{O}_{\pm}}(\mu)$. We have, from (22),

$$\gamma_{\pm}(g_s) \equiv \mu \frac{\partial \log Z_{\mathcal{O}_{\pm}}(\mu)}{\partial \mu} = \mu \frac{\partial \log c_{\pm}(\mu)}{\partial \mu} = - \left[d_{\pm} \frac{\alpha_s(\mu)}{\pi} \right]. \quad (16.24)$$

The fact that the product $c_{\pm}(\mu) \mathcal{O}_{\pm}^{\text{ren}}(\mu) = \mathcal{O}_{\pm}^{\text{bare}}$ is independent of μ implies

$$\left\{ \mu \frac{d}{d\mu} + \gamma_{\pm} \right\} \mathcal{O}_{\pm}^{\text{ren}}(\mu) = 0, \quad \left\{ \mu \frac{d}{d\mu} - \gamma_{\pm} \right\} c_{\pm}(\mu) = 0.$$

The latter may be rewritten as

$$\frac{d}{d \log(\mu/M_W)} c_{\pm}(\mu) = \gamma_{\pm}(g_s) c_{\pm}(\mu), \quad (16.25)$$

with the initial condition $c_{\pm}(M_W) = 1$. This differential equation is easy to solve. When we put into (25) the explicit expression (24) of $\gamma_{\pm}(g_s)$ written in terms of the QCD running coupling $\alpha_s(\mu)$ as given by (15.83), i.e.

$$\alpha_s(\mu) = \frac{2\pi}{b_0 \log(\mu/\Lambda_{\overline{\text{MS}}})}, \quad \text{where } b_0 = \frac{11}{3}N_c - \frac{2}{3}N_f,$$

then we find that the solutions of (25) are

$$\begin{aligned} c_{\pm}(\mu) &= \left[\frac{\log(M_W/\Lambda_{\overline{\text{MS}}})}{\log(\mu/\Lambda_{\overline{\text{MS}}})} \right]^{2d_{\pm}/b_0} = \left[\frac{\alpha_s(\mu)}{\alpha_s(M_W)} \right]^{2d_{\pm}/b_0} \\ &= \left[1 + b_0 \frac{\alpha_s(\mu)}{4\pi} \log \frac{M_W^2}{\mu^2} \right]^{2d_{\pm}/b_0}. \end{aligned} \quad (16.26)$$

This expression of $c_{\pm}(\mu)$ manifestly represents the summation of the series $\sum[\alpha_s \log(M_W/\mu)]^n$. It is gratifying to check that for $\alpha_s \ll 1$ we recover (22):

$$\left[1 + b_0 \frac{\alpha_s(\mu)}{4\pi} \log \frac{M_W^2}{\mu^2}\right]^{2d_{\pm}/b_0} \xrightarrow{\alpha_s \ll 1} 1 + d_{\pm} \left\{ \frac{\alpha_s(\mu)}{\pi} \log \frac{M_W}{\mu} \right\}.$$

The renormalization group analyses replace the $c_{\pm}(\mu)$ in (22) with the new expressions in (26):

$$\begin{aligned} c_+ &= 1 - \frac{\alpha_s}{\pi} \log \left(\frac{M_W}{\mu} \right) \Rightarrow \left[\frac{\alpha_s(\mu)}{\alpha_s(M_W)} \right]^{-2/b_0}, \\ c_- &= 1 + 2 \frac{\alpha_s}{\pi} \log \left(\frac{M_W}{\mu} \right) \Rightarrow \left[\frac{\alpha_s(\mu)}{\alpha_s(M_W)} \right]^{+4/b_0}. \end{aligned} \quad (16.27)$$

Renormalized by QCD according to (19), the original \mathcal{O}_A in (3) now becomes the new $\mathcal{O}_{NL} = c_+ \mathcal{O}_+ + c_- \mathcal{O}_-$ which constitutes the effective Lagrangian for nonleptonic decays:

$$\begin{aligned} \mathcal{O}_A &\Rightarrow \mathcal{O}_{NL} = c_+ \mathcal{O}_+ + c_- \mathcal{O}_- = c_A \mathcal{O}_A + c_B \mathcal{O}_B, \\ \mathcal{O}_{\pm} &= \frac{1}{2} \{ [\bar{c}\gamma^\mu(1-\gamma_5)b] [\bar{d}\gamma_\mu(1-\gamma_5)u] \pm [\bar{c}\gamma^\mu(1-\gamma_5)u] [\bar{d}\gamma_\mu(1-\gamma_5)b] \}, \\ c_A &= \frac{1}{2}(c_+ + c_-), \quad c_B = \frac{1}{2}(c_+ - c_-). \end{aligned} \quad (16.28)$$

We note that $(c_+)^2 = 1/c_-$, and $c_+ < 1 < c_-$ for all scales μ . The operator \mathcal{O}_- receives an enhancement by c_- , while the \mathcal{O}_+ is suppressed by c_+ . From (3) to (28), the important result

$$H^\mu H_\mu^\dagger \Rightarrow \sum c_n \mathcal{O}_n$$

which illustratesⁿ the Wilson operator product expansion (OPE) method, is the starting point of all phenomenological analyses of inclusive as well as exclusive hadronic decays, and will be extensively used in the next sections.

16.1.4 The $\Delta I = \frac{1}{2}$ in Strangeness Hadronic Decays

As the first application, the general result (28) is now used to study nonleptonic decays of strange particles described by $s \rightarrow u + d + \bar{u}$. Historically, the works on QCD renormalization² of weak interaction were motivated by this $\Delta I = \frac{1}{2}$ empirical rule (Chap. 6). We start from

$$\frac{G_F}{\sqrt{2}} V_{us} V_{ud}^* [\bar{d}\gamma^\mu(1-\gamma_5)u] [\bar{u}\gamma_\mu(1-\gamma_5)s] \equiv \frac{G_F}{\sqrt{2}} V_{us} V_{ud}^* \mathcal{O}_A^{S=1}, \quad (16.29)$$

where $\mathcal{O}_A^{S=1}$ is an equal mixture of the $I = 1/2, 3/2$ isospin components.

² Gaillard, M. K. and Lee, B. W., Phys. Rev. Lett. **33** (1974) 108; Altarelli, G. and Maiani, L., Phys. Lett. **52B** (1974) 351

Indeed, the s field is an isoscalar ($I = 0$) object (as all other flavored quarks), only the unflavored u, d fields form an isospin doublet. Therefore the $\bar{d}\gamma^\mu(1-\gamma_5)u$ current behaves as an $I = 1$ operator (since $I_3 = 1$), whereas the other current $\bar{u}\gamma_\mu(1-\gamma_5)s$ has $I = 1/2$. The product $1 \otimes 1/2$ of the two isospin currents is a mixture of isospin $1/2 \oplus 3/2$. A priori, the nonleptonic operator $\mathcal{O}_A^{S=1}$ described by the product of these two currents can have the component $I = 3/2$ as important as the $I = 1/2$ component; they are on the same footing.

This isospin analysis strongly disagrees with experiments. As explained in Chap. 6, the isospin $I = 1/2$ part of all nonleptonic decay amplitudes largely dominates the $I = 3/2$ component. Nonleptonic weak decays of strange particles (the mesons K as well as the hyperons $\Lambda, \Sigma, \Xi, \Omega^-$) regularly obey the $\Delta I = 1/2$ rule, the ratio $(A_{1/2})/(A_{3/2})$ of the decay amplitudes ranges between 15–30, i.e. the corresponding $\Delta I = 1/2$ rates are a few hundred times faster than the rates having only the $\Delta I = 3/2$ like the $K^+ \rightarrow \pi^+ + \pi^0$ mode.

Let us indicate how QCD partially solves this difficult problem which has been with us since the 1950s and is still not completely understood at present. From (28) the ‘tree’ operator $\mathcal{O}_A^{S=1}$ in (29) gets renormalized by QCD and becomes

$$\mathcal{O}_A^{S=1} \Rightarrow c_- \mathcal{O}^{(\frac{1}{2})} + c_+ \mathcal{O}^{(\frac{3}{2})}.$$

We identify \mathcal{O}_-^S with $\mathcal{O}^{(\frac{1}{2})}$ and \mathcal{O}_+^S with $\mathcal{O}^{(\frac{3}{2})}$. The subscripts $\frac{1}{2}$ and $\frac{3}{2}$ refer to the isospin content of these operators. Let us first show that \mathcal{O}_-^S is a pure $I = 1/2$ operator. Indeed

$$\mathcal{O}_-^S = \frac{1}{2} \left\{ [\bar{d}\gamma^\mu(1-\gamma_5)u] [\bar{u}\gamma_\mu(1-\gamma_5)s] - [\bar{u}\gamma^\mu(1-\gamma_5)u] [\bar{d}\gamma_\mu(1-\gamma_5)s] \right\}$$

is antisymmetric under the interchange of $\bar{u} \leftrightarrow \bar{d}$. The antisymmetric state of these \bar{u} and \bar{d} fields has total isospin $I = 0$, so that the whole \mathcal{O}_-^S is purely an $I = 1/2$ object. The $I = 1/2$ structure of \mathcal{O}_-^S can also be recognized by using the raising I_+ and lowering I_- isospin operators defined by

$$I_+ d = u, \quad I_+ \bar{u} = -\bar{d}, \quad I_- u = d, \quad I_- \bar{d} = -\bar{u}.$$

When applying I_+ on \mathcal{O}_-^S , we find $I_+ \mathcal{O}_-^S = 0$. Since \mathcal{O}_-^S has $I_3 = +\frac{1}{2}$, this implies that the total isospin I of \mathcal{O}_-^S must be $1/2$, otherwise we would not get a vanishing result with the raising I_+ operator. On the other hand, \mathcal{O}_+^S is a mixture of $I = 1/2$ and $I = 3/2$ since by applying the lowering operator I_- on \mathcal{O}_+^S , one gets $I_- \mathcal{O}_+^S \neq 0$.

QCD renormalization of the weak operator $\mathcal{O}_A^{S=1}$ in (29) enhances the $I = 1/2$ part and suppresses the $I = 3/2$ part. At the scale $\mu = m_K$ of K decays and using (27), the associated coefficients are $c_-(m_K) = 2.1$ and

$c_+(m_K) = 0.7$. The $\Delta I = 1/2$ enhancement (by the coefficient c_-) over the $\Delta I = 3/2$ suppression (by the coefficient c_+) is about 3. This is encouraging but not large enough. For instance, in $K \rightarrow \pi + \pi$, the ratio $(A_{1/2})/(A_{3/2})$ is found to be ≈ 22 (see Chap. 11).

To obtain the decay amplitude A_I , in addition to the coefficients c_- and c_+ , we also need the matrix elements of the associated operators \mathcal{O}_-^S and \mathcal{O}_+^S inserted between the hadronic states K and $\pi + \pi$. This part is determined by nonperturbative QCD dynamics of the light K and π mesons which is likely governed by the chiral symmetry. This topic is not covered in this book. Quantitatively, it is not clear how $c_- \langle \pi\pi | \mathcal{O}_- | K \rangle$ could dominate $c_+ \langle \pi\pi | \mathcal{O}_+ | K \rangle$ by a factor of 22.

Finally, we mention that the penguin operator (11.93) arising from QCD corrections has also the dimension six as $\mathcal{O}_A^{S=1}$ and $\mathcal{O}_B^{S=1}$, so it can mix with them too. The penguin operator is not of a $(V - A) \times (V - A)$ type as are $\mathcal{O}_A^{S=1}$ and $\mathcal{O}_B^{S=1}$, rather it has the structure $V \times (V - A)$. The mixing is not as simple as the $\mathcal{O}_\pm^{S=1}$ in (21) since we cannot use the Fierz rearrangement together with (11.88). The final result³ is that there are four additional terms related to gluonic penguin and four to electroweak penguin (diagrams with photon and Z^0 replacing the gluon), so in total there are ten operators instead of two, $\mathcal{O}_A^{S=1}$ and $\mathcal{O}_B^{S=1}$. As emphasized in Chap. 11, the gluonic penguin is also a pure $I = 1/2$ operator. Due to the Fierz transformation $V \times (V - A) \sim S + P$ (see the Appendix), its matrix element taken between the K and 2π states may be arranged into $\langle 0 | P | K \rangle$, $\langle \pi | P | 0 \rangle$, and $\langle \pi | S | K \rangle$. These quantities are proportional to $1/m_s$ and $1/m_d$ so they can be large for light quark masses m_s and m_d (Problem 16.1). However, the coefficients associated with these penguin matrix elements are small, and the overall contributions may not be sufficiently large.

In brief, the $\Delta I = 1/2$ rule is still an open question and only semiquantitatively understood. Presumably because the s quark is not heavy, we are in the low-energy regime of strangeness decay, for which nonperturbative QCD effect is important and should be included. On the other hand, for heavy particles, perturbative QCD is more reliable due to asymptotic freedom.

16.2 Heavy Flavor Symmetry

Mesons as bound states of quarks and antiquarks can be grouped into three categories $q\bar{q}$, $Q\bar{Q}$ and $Q\bar{q}$ where q stands for light u , d , or s quarks while Q for heavy c or b (the top is too heavy to form hadronic bound states before it decays).

These bound states are characterized by a large separation of mass scales: $M_Q \approx \text{few GeV}$ and $\Lambda_{\text{QCD}} \equiv \Lambda_{\overline{MS}} \approx 0.2 \text{ GeV}$, or equivalently, of length scales

³ Buras, A. J., Jamin, M., Lautenbacher, M. E. and Weisz, P. H., Nucl. Phys. **B370** (1992) 69; *ibid* **B375** (1992) 501. Adel, K. and Yao, Y. P., Phys. Rev. **D49** (1994) 4945.

$\lambda_Q \simeq 1/M_Q$ and $R_{\text{had}} \simeq 1/\Lambda_{\text{QCD}}$. The sizes of $q\bar{q}$ or $Q\bar{q}$ hadrons are more or less determined by $R_{\text{had}} \approx 1$ fm which sets the nonperturbative confining regime of quarks and gluons.

On the other hand, the QCD coupling $\alpha_s(M_Q)$ of heavy quarks is small due to the asymptotic freedom, implying that on length scales comparable to $\lambda_Q \ll R_{\text{had}}$, the strong interaction is similar to the electromagnetic interactions. Presumably, for this reason the quarkonium system $Q\bar{Q}$, whose size is of the order of $\lambda_Q/\alpha_s(M_Q) \ll R_{\text{had}}$, behaves like the positronium (Chap. 7).

16.2.1 Basic Physical Pictures

At first sight a heavy hadron, say a meson $Q\bar{q}$, seems to be more difficult to treat because its size is still determined by the long-distance confining regime $\sim R_{\text{had}}$ on the one hand, while the Compton wavelength λ_Q of the heavy quark is much smaller on the other hand.

However, the crucial point is that the typical momenta exchanged between the light constituents (\bar{q} , gluons) and the heavy quark Q are only of the order Λ_{QCD} in the confining state $Q\bar{q}$. An energetic hard probe would be required to resolve the properties of the heavy quark Q (for instance its flavors and its spin orientations). The soft momenta exchanged between the light constituents and the heavy Q can only probe distances much larger than λ_Q . Therefore, to the extent that charm and bottom are considered heavy, the light constituents of the mesons $Q\bar{q}$ are *insensitive* to the flavor (charm or bottom), mass (M_c or M_b), and spin orientations of the heavy quark Q .

The heavy Q acts as a static source of color electric field localized at the origin, relativistic effects such as color magnetism vanish as $M_Q \rightarrow \infty$. Therefore, the spin of Q decouples, and the light quark and gluon cannot recognize the spin orientations of Q . This is completely different from the situation found in $q\bar{q}$ and $Q\bar{Q}$ systems. The irrelevant effect of M_Q on the properties of $Q\bar{q}$ can be seen as follows. In the rest frame of the heavy hadron, the heavy quark Q is at rest too, and it is almost on its mass-shell. The wave function of the light constituents follows from a solution of the field equations of QCD subject to the boundary condition of the *static color source* Q . This boundary condition is independent of M_Q , and so is the solution of the light constituents. This is the physical picture of the heavy flavor symmetry (HFS) concerning both flavors and spins of the heavy quarks.

The situation bears some similarity with atoms where the nucleus plays the role of Q and the surrounding electrons that of \bar{q} . Various isotopes of a given atomic element have, to a good approximation, the same chemical properties. Since the electron is governed only by the total electric charge of the nucleus, adding some neutrons to or removing some from the nucleus may not change its chemistry. The equivalent of the isotopes are the mesons B , D , B^* , D^* , and the baryons Λ_b , Λ_c . Their light constituents cannot distinguish their heavy partners Q in the limit $M_Q \rightarrow \infty$. The spin symmetry is analogous to the degenerate hyperfine levels in atoms.

Although, for the moment, this observation still does not allow any concrete calculation, and since M_Q is not infinite, corrections to large but finite M_Q must be somehow treated, the idea nevertheless provides some interesting relations between the properties of such particles and can be experimentally checked. This is illustrated by the following examples.

Spectroscopic Consequences of HFS. In the limit $M_Q \rightarrow \infty$, the spin of the heavy quark and the total angular momentum j of the light degrees of freedom inside a hadron are decoupled. The mass M_Q is irrelevant, the dynamics is independent of the spin and mass of the heavy quark. Heavy flavored hadronic states can thus be characterized by the light flavor, spin, parity of the light constituents. The heavy flavor symmetry relates the properties of different bottom and charm particles, while the spin symmetry predicts that, for a fixed $j \neq 0$, there is a doublet of degenerate states with total spin $J = j \pm \frac{1}{2}$.

In general, the mass of a hadron H_Q containing a heavy quark Q can be written in the form

$$M_H = M_Q + \bar{\Lambda}_q + \frac{\Delta m^2}{2M_Q} + \mathcal{O}(1/M_Q^2), \quad (16.30)$$

where the parameter $\bar{\Lambda}_q$ represents contributions arising from all terms in the effective Lagrangian that are independent of M_Q , while Δm^2 originates from all terms of order $1/M_Q$. For the moment, the details of these terms are not important, they will be determined later by the Heavy Quark Effective Theory (HQET). For the ground states $J^P = 0^-$ and $J^P = 1^-$, one can parameterize the Δm^2 in terms of the two quantities λ_1 and λ_2 ,

$$\Delta m^2 = \lambda_1 + 2[J(J+1) - \frac{3}{2}]\lambda_2, \quad (16.31)$$

where J is the total spin of the meson H_Q . All parameters $\bar{\Lambda}_q, \lambda_1, \lambda_2$ are independent of M_Q , they are functions of the light constituents. So

$$M_{B_s} - M_{B_d} = \bar{\Lambda}_s - \bar{\Lambda}_d + \mathcal{O}(1/M_b), \quad M_{D_s} - M_{D_d} = \bar{\Lambda}_s - \bar{\Lambda}_d + \mathcal{O}(1/M_c),$$

where the value of $\bar{\Lambda}_q$ depends on the light constituents collectively denoted by q in (30). Since both charm and bottom are considered as heavy, the mass splitting should be equal. It is confirmed by experiments:

$$M_{B_s} - M_{B_d} = 90 \pm 3 \text{ MeV} \quad \text{and} \quad M_{D_s} - M_{D_d} = 99 \pm 1 \text{ MeV}.$$

For the pseudoscalar and vector meson mass splitting, from (31), we get

$$M_{B^*}^2 - M_B^2 = 4\lambda_2 + \mathcal{O}(1/M_b) \quad \text{and} \quad M_{D^*}^2 - M_D^2 = 4\lambda_2 + \mathcal{O}(1/M_c). \quad (16.32)$$

Again this prediction is compatible with data, which give

$$M_{B^*}^2 - M_B^2 \simeq 0.49 \text{ GeV}^2 \quad \text{and} \quad M_{D^*}^2 - M_D^2 \simeq 0.55 \text{ GeV}^2. \quad (16.33)$$

16.2.2 Elements of Heavy Quark Effective Theory (HQET)

The Fermi theory of weak interactions represented by the right-hand side of (3) is a typical example of an effective Lagrangian. The W weak boson effect is ‘integrated out’ and replaced by the dimensional coupling G_F and calculations can be done at low energies far below the W mass. In this effective Fermi theory, we only use G_F . Neither the fundamental weak coupling g nor the W mass are considered in the computation. Physical quantities computed from the effective theory are the same as if they are calculated with the fundamental Lagrangian in a certain kinematic region. It is only at much higher energies that the W^\pm and Z^0 effects can be felt, and the difference appears. We have met one example: the neutrino cross-section (12.43) approximates at low energies the exact results (12.42) and (12.44) derived from the fundamental Lagrangian with the full weak boson effects.

A similar calculational method may be formulated within HQET as a systematic expansion in terms of local operators with powers of Λ_{QCD}/M . The long-distance physics of several observables is described by a few parameters which can be defined and calculable in terms of the matrix elements of these operators.

The starting point is the *velocity* v^μ of the heavy hadron H defined by $M_H v^\mu = P^\mu$, where M_H and P^μ are the mass and four-momentum of H containing the heavy quark Q. We note that $v^2 = v^\mu v_\mu = 1$.

To construct an effective theory in which the heavy quark mass M (we drop the index Q) becomes irrelevant, we let M tend to infinity while keeping fixed the four-velocity as in classical mechanics. The momentum P_Q^μ of the heavy quark may be written as

$$P_Q^\mu = M v^\mu + k^\mu, \quad (16.34)$$

where k^μ is much smaller than $M v^\mu$. The heavy quark is almost on-mass-shell, i.e. $P_Q^2 \approx M^2$. Consider the transition of the hadron H into a new state of the same heavy quark (with velocity v') and k^μ is the momentum transfer. The transition changes the residual momentum $\delta k \sim \Lambda_{\text{QCD}}$, but the changes in the heavy quark velocity $\delta v = v - v'$ vanish as $\Lambda_{\text{QCD}}/M \rightarrow 0$, i.e. the velocity v^μ is a conserved quantity.

The next step is to introduce the large component $H_v(x)$ and small component $h_v(x)$ of the quark field $Q(x)$ by

$$Q(x) = e^{-iMv \cdot x} [H_v(x) + h_v(x)], \quad (16.35)$$

$$H_v(x) = e^{iMv \cdot x} \mathcal{P}_+ Q(x), \quad h_v(x) = e^{iMv \cdot x} \mathcal{P}_- Q(x), \quad (16.36)$$

where \mathcal{P}_\pm are the projection operators defined as

$$\mathcal{P}_\pm = \frac{1 \pm \not{v}}{2} \quad \text{with} \quad \not{v} = \gamma_\mu v^\mu. \quad (16.37)$$

The main dependence on M has been factored out and contained in the exponential. These new fields satisfy $\not{v}H_v = H_v$ and $\not{v}h_v = -h_v$.

The heavy quark moving with a fixed velocity has its wave function essentially contained in H_v . Compared to H_v , the component h_v is suppressed by Λ_{QCD}/M and is absent for an on-shell heavy quark Q . Recall that in the Dirac equation (Chap. 3), there are the two-component upper and lower parts of the full four-component spinor [see (3.45)]. The large and small components are respectively the upper and lower parts of the full four-component spinor of Q in the rest frame $v^\mu = (1, 0, 0, 0)$. The field H_v destroys a heavy quark, while h_v creates a heavy antiquark with the same velocity v .

The QCD Lagrangian quark–gluon interaction $\mathcal{L}_Q = \bar{Q}(\not{D} - M)Q$ is now rewritten in terms of the new large and small components H_v and h_v :

$$\begin{aligned} \mathcal{L}_Q = & \bar{H}_v(\not{v} \cdot D) H_v - \bar{h}_v(\not{v} \cdot D + 2M)h_v \\ & + [\bar{H}_v(\not{D}_\perp) h_v + \bar{h}_v(\not{D}_\perp) H_v] , \end{aligned} \quad (16.38)$$

where D^μ is the QCD covariant derivative, and $D_\perp^\mu = D^\mu - (v \cdot D)v^\mu$ is orthogonal to the velocity, i.e. $v \cdot D_\perp = 0$.

Clearly, H_v describes massless degrees of freedom, while h_v corresponds to fluctuations with mass twice the mass M . The h_v , representing the heavy degrees of freedom, will be eliminated in the construction of HQET. Using the equation of motion $(\not{D} - M)Q = 0$, we can re-express h_v in terms of H_v . Indeed,

$$h_v = \left[\frac{\not{D}_\perp}{2M + \not{v} \cdot D} \right] H_v ,$$

which shows that the small component h_v is of order $1/M$. The above equation is now put back into (38), and we get a nonlocal effective Lagrangian

$$\mathcal{L}_{\text{eff}} = \bar{H}_v(\not{v} \cdot D) H_v + \bar{H}_v(\not{D}_\perp) \frac{1}{2M + \not{v} \cdot D} (\not{D}_\perp) H_v .$$

Because of the phase factor in (36), the x dependence of the effective field H_v is weak. In momentum space, derivatives acting on H_v represent powers of the residual momentum k^μ which are smaller than M . Therefore, the nonlocal Lagrangian can be expanded in powers of \not{D}/M :

$$\mathcal{L}_{\text{eff}} = \bar{H}_v(\not{v} \cdot D) H_v + \frac{1}{2M} \sum_{n=0}^{\infty} \bar{H}_v(\not{D}_\perp) \left[-\frac{\not{v} \cdot D}{2M} \right]^n (\not{D}_\perp) H_v .$$

Since $\mathcal{P}_+(\not{D}_\perp)(\not{D}_\perp)\mathcal{P}_+ = \mathcal{P}_+ \left\{ (\not{D}_\perp)^2 + \frac{g_s}{2} \sigma_{\mu\nu} G^{\mu\nu} \right\} \mathcal{P}_+$,

with $[iD^\mu, iD^\nu] = ig_s G^{\mu\nu}$ is the gluon field-strength tensor, one finds

$$\mathcal{L}_{\text{eff}} = \bar{H}_v(\not{v} \cdot D) H_v + \frac{1}{2M} \bar{H}_v(\not{D}_\perp)^2 H_v + \frac{g_s}{4M} \bar{H}_v(\sigma_{\mu\nu} G^{\mu\nu}) H_v + \dots , \quad (16.39)$$

where the dots represents $\mathcal{O}(\frac{1}{M^2})$. The first term

$$\overline{H}_v (i v \cdot D) H_v \quad (16.40)$$

clearly indicates that the strong interaction of a heavy quark is independent of its mass and spin. Since the Dirac matrices are absent, interactions of the heavy quark with gluons leave its spin unchanged. If there are N_H heavy quarks moving with the same velocity v , then (40) is generalized to

$$\sum_{j=1}^{N_H} \overline{H}_v^j (i v \cdot D) H_v^j .$$

Its invariance under the rotation in flavor space is manifest. When combined with the spin symmetry, we get the $SU(2N_H)$ group which represents the spin and heavy flavor symmetries. Coming from the $1/M$ expansion, corrections to the spectator model are provided by the two other terms in (39).

The second operator

$$\mathcal{O}_{\text{kin}} = \frac{1}{2M} \overline{H}_v (i \not{D}_\perp)^2 H_v \longrightarrow -\frac{1}{2M} \overline{H}_v (i \mathbf{D})^2 H_v$$

is the gauge-covariant generalization of the kinetic energy arising from the residual motion of the nearly on-mass-shell heavy quark Q . In the rest frame of the heavy particle H , $(i \mathbf{D})^2 = (i v_\mu D^\mu)^2 - (i D_\mu)(i D^\mu)$ is the square of the operator representing the spatial momentum of the heavy quark.

Analogous to the Pauli magnetic interaction, the third operator describes the chromomagnetic coupling of the heavy quark spin to the gluon field

$$\mathcal{O}_{\text{mag}} = \frac{g_s}{4M} \overline{H}_v (\sigma_{\mu\nu} G^{\mu\nu}) H_v \longrightarrow -\frac{g_s}{M} \overline{H}_v (\mathbf{S} \cdot \mathbf{B}_{gl}) H_v ,$$

where $\mathbf{S} = \frac{1}{2} \boldsymbol{\sigma}$ is the spin operator (σ^i are the three Pauli matrices), and the space components of the chromomagnetic field \mathbf{B}_{gl} are $B_{gl}^i = -\frac{1}{2} \epsilon^{ijk} G_{jk}$. The three terms in (39) constitute the basis for the computation of decay rates, in particular of the inclusive widths of heavy flavored hadrons. In the limit $M \rightarrow \infty$, only (40) remains and represents HQET.

16.3 Inclusive Decays

As the first application of HQET, let us calculate the two typical inclusive decays of a heavy particle, say of the \overline{B} meson taken as an example: the semileptonic Γ_{SL} and the nonleptonic Γ_{NL} widths

$$\Gamma_{\text{SL}} \equiv \Gamma(\overline{B} \rightarrow \ell^- + \overline{\nu}_\ell + \text{hadrons}) \quad \text{and} \quad \Gamma_{\text{NL}} \equiv \Gamma(\overline{B} \rightarrow \text{hadrons}) .$$

By definition, hadrons are not identified in these inclusive modes. Neglecting some rare decay modes like $\overline{B} \rightarrow \gamma + \overline{K}^*$ (issued from higher-order penguin

loop diagram $b \rightarrow s + \gamma$), the sum of these inclusive decays saturates the total width or the inverse of the \bar{B} meson lifetime. The latter by definition describes the most inclusive decay one can imagine, since none of the particles in the final state is observed. Inclusive semileptonic decays are relatively easy to measure, only the charged lepton ℓ^- is identified in the decay product. The inclusive nonleptonic rate may be obtained by subtraction from the total width the sum over $\ell^- = e^-, \mu^-, \text{ and } \tau^-$ of the inclusive Γ_{SL} .

From the theoretical viewpoint, inclusive decays of heavy hadrons have two unique features. First, bound-state effects related to the decaying \bar{B} such as the motion of the heavy b quark inside the initial state can be systematically accounted for by using the $1/M$ expansion. The leading term describes the free b quark decay, i.e. the spectator parton model. Secondly, since the final states contain so many hadrons in all possible channels, the bound-state effects of individual decay products may be eliminated (more exactly averaged out). This situation of course does not hold for light hadrons which have a very limited number of decay products. The second property is based on a concept called quark-hadron duality, a typical example of which is the inclusive semileptonic decays of the heavy lepton τ discussed in Chap. 13.

According to the quark-hadron duality, the inclusive decay rate is calculable by QCD, i.e. at the quark and gluon level, after a smearing (or averaging) procedure has been applied. In semileptonic decays $\bar{B} \rightarrow \ell^- + \bar{\nu}_\ell + X$, the integration over the lepton pair phase space provides a smearing over the invariant mass squared $(P_B - q)^2$ of the hadrons X , where $q = p_\ell + p_{\nu}$. In $\tau \rightarrow \nu_\tau + X$, the integration over the ν_τ momentum provides the smearing.

16.3.1 General Formalism

From the optical theorem, the inclusive decay rate of the meson \bar{B} may be obtained from the imaginary part of the forward transition amplitude $\bar{B} \rightarrow \bar{B}$ to second-order G_F^2 as shown by Fig. 16.6. The inclusive width can be written as

$$\Gamma(\bar{B} \rightarrow X) = \frac{1}{2M_B} \{2 \operatorname{Im} \langle \bar{B} | \mathbf{T} | \bar{B} \rangle\} . \quad (16.41)$$

The operator \mathbf{T} is given by

$$\mathbf{T} = i \int d^4x T \{ \mathcal{L}_W(x), \mathcal{L}_W(0) \} . \quad (16.42)$$

Inserting a complete set of states X in the time-ordered T product, we recover the standard formula for the decay rate:

$$\Gamma(\bar{B} \rightarrow X) = \frac{1}{2M_B} \sum_X (2\pi)^4 \delta^4(P_B - P_X) |\langle X | \mathcal{L}_W | \bar{B} \rangle|^2 . \quad (16.43)$$

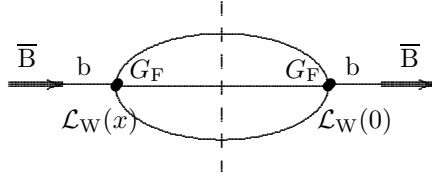


Fig. 16.6. Imaginary part of the forward scattering amplitude $\bar{B} \rightarrow \bar{B} \iff$ Decay rate of $b \rightarrow X \rightarrow b$, to order G_F^2 . Dashed line cut gives the imaginary part

In (42), $\mathcal{L}_W(x)$ is the effective weak Lagrangian built up from the quark fields and corrected by QCD as outlined in Sect. 16.1. Most importantly, the $b(x)$ quark field in $\mathcal{L}_W(x)$ is governed by the HQET Lagrangian.

Because of the large b quark mass, the momenta flowing through the internal lines in the diagram of Fig. 16.6 are large, thus, following the Wilson operator product expansion method, the nonlocal operator \mathbf{T} may be represented as a sum of local operators $\sum_n \mathcal{O}_n(b)$ containing the $b(x)$. The decay rate may therefore be written as

$$\Gamma(\bar{B} \rightarrow X) = \frac{G_F^2 M^5}{192\pi^3} \sum_n a_n(b \rightarrow X) \frac{1}{2M_B} \langle \bar{B} | \mathcal{O}_n(b) | \bar{B} \rangle. \quad (16.44)$$

On the right-hand side of the above equation, the first common factor $\Gamma_0 = G_F^2 M^5 / 192\pi^3$ represents the free heavy quark b decay width as given by the spectator model symbolically depicted in Fig. 16.1. The coefficient $a_n(b \rightarrow X)$ appropriately specifies the mode in which the b quark decays into a definite final state X , e.g. the semileptonic or the nonleptonic mode. The last factor $\frac{1}{2M_B} \langle \bar{B} | \mathcal{O}_n(b) | \bar{B} \rangle$ parameterizes the long-distance bound-state effect of the b quark inside the \bar{B} meson. The $1/2M_B$ coefficient is conveniently introduced for dimensional reason, as can be seen later in (53). HQET allows us to determine the last factor by an expansion in powers of $1/M$, the leading term is model independent and represented by (53).

By a simple dimensional argument, operators $\mathcal{O}_n(b)$ with higher dimension are suppressed by higher powers of $1/M$. Constructed from the b quark and gluon fields, and since $\mathcal{O}_n(b)$ is a scalar object by definition, the operator having the lowest dimension is $\bar{b}b$ with dimension 3. The next operators of dimension 4 are absent. The reason is simple, since the only gauge-invariant operator of dimension $d = 4$ is $\bar{b}(i \not{D})b$. However, when inserted between physical quark states, this operator can be reduced to $M\bar{b}b$ using the equation of motion of the b field. The next-to-leading operator of dimension $d = 5$ is the one with the gluon field $g_s \bar{b}(\sigma_{\mu\nu} G^{\mu\nu})b$. So we have

$$\sum_n \mathcal{O}_n(b) = \bar{b}b + \frac{1}{M^2} g_s \bar{b}(\sigma_{\mu\nu} G^{\mu\nu})b + \mathcal{O}\left(\frac{1}{M^3}\right). \quad (16.45)$$

We proceed in two steps to calculate the inclusive rate $\Gamma(\bar{B} \rightarrow X)$ from (44). The first step concerns the coefficients $a_n(b \rightarrow X)$; they are considered at the

quark level. For instance, the inclusive semileptonic decays are described by $b \rightarrow q_1 + \ell^- + \bar{\nu}_\ell$, where q_1 stands for the charm and the up quarks. As for the inclusive nonleptonic decays, we compute $b \rightarrow q_1 + q_2 + \bar{q}_3$, where the $q_2\text{--}\bar{q}_3$ pair stands for $d\text{--}\bar{u}$ and $s\text{--}\bar{c}$ (Cabibbo-favored modes due to $|V_{ud}| \approx |V_{cs}| \approx 1$) or $s\text{--}\bar{u}$ and $d\text{--}\bar{c}$ (Cabibbo-suppressed reactions, $|V_{us}| \approx |V_{cd}| \approx 0.22$).

The second step concerns the matrix elements of the two operators $\bar{b}b$ and $\bar{b}\sigma_{\mu\nu}G^{\mu\nu}b$ in (45) inserted between the \bar{B} states. The operator $\bar{b}b$ dominates over the second $\bar{b}\sigma_{\mu\nu}G^{\mu\nu}b$ by $1/M^2$, so let us first concentrate on the former. Using (39), we develop the $\bar{b}\not{v}b$ as another series in inverse powers of M :

$$\bar{b}\not{v}b = \bar{b}b + \frac{1}{2M^2}\bar{b}[(iv \cdot D)^2 - (iD)^2]b - \frac{1}{2M^2}\bar{b}\left[\frac{1}{2}g_s\sigma_{\mu\nu}G^{\mu\nu}\right]b + \dots, \quad (16.46)$$

where the dots represent the $\mathcal{O}(1/M^3)$ terms. The important thing is that the matrix element of the left-hand side of (46) inserted between the physical \bar{B} meson states is definitely known. Actually, the $\bar{b}\gamma^\mu b$ is the Noether current for the global bottom quantum number, its expectation value is thus determined by the bottom flavor content of the \bar{B} meson and must be 1. This can be seen as follows.

The starting point is the elastic transition of a \bar{B} meson of velocity v into another \bar{B} meson of velocity v' induced by the vector current $\bar{b}\gamma^\mu b$ of the HQET $b(x)$ field. The most general form of this transition is

$$\frac{1}{M_B}\langle \bar{B}(v') | \bar{b}\gamma^\mu b | \bar{B}(v) \rangle = \xi(v \cdot v') (v + v')^\mu, \quad (16.47)$$

where the dimensionless quantity $\xi(v \cdot v')$ is called the Isgur–Wise function. The factor $1/M_B$ on the left-hand side compensates for the dimensional dependence on $(\text{mass})^{-1}$ of the state $|\bar{B}\rangle$ in the conventional one-particle state normalization

$$\langle \bar{B}(p') | \bar{B}(p) \rangle = 2M_B v^0 (2\pi)^3 \delta^3(\mathbf{p} - \mathbf{p}'). \quad (16.48)$$

There is no term proportional to $(v - v')^\mu$ on the right-hand side of (47), as can be seen by contracting its left-hand side with $(v - v')^\mu$ and noting that $\not{v}b_v = b_v$ and $\bar{b}_{v'}\not{v}' = \bar{b}_{v'}$.

The form (47) is familiar, we have met it in (10.11) with the electromagnetic form factor $F_\pi(q^2)$ of the π meson which has an identical Lorentz structure. Like (10.11), the matrix element of the vector current $\bar{b}\gamma^\mu b$ – inserted between the \bar{B} meson states – defines the \bar{B} meson electromagnetic form factor $F_B(q^2)$:

$$\langle \bar{B}(v') | \bar{b}\gamma^\mu b | \bar{B}(v) \rangle = F_B(q^2)(p + p')^\mu, \quad (16.49)$$

where $p^\mu = M_B v^\mu$, $p'^\mu = M_B v'^\mu$. Comparing (49) with (47), one gets

$$F_B(q^2) = \xi(v \cdot v'), \text{ where } q^2 = (p - p')^2 = 2m_B^2(1 - v \cdot v'). \quad (16.50)$$

As emphasized in (10.11), the form factor is normalized to unity at $q^2 = 0$ since the current is conserved. This normalization at, and only at $q^2 = 0$, is not modified by strong or electroweak interaction. This is the physical reason for the charge of the electron to be the same as that of the charged \bar{B} meson (or the antiproton) for instance. Although they are governed by completely different interactions, their electric charges are identical, i.e. their electromagnetic form factors at $q^2 = 0$ are all equal to unity:

$$F_B(0) = F_D(0) = F_K(0) = F_\pi(0) = F_1^P(0) = 1. \quad (16.51)$$

From (50) and (51), we get

$$\xi(\omega = 1) = 1, \quad \text{where } \omega \equiv v \cdot v'. \quad (16.52)$$

The model-independent normalization $\xi(1) = 1$ turns out to be very useful for the determination of many weak-interaction form factors involved in heavy flavor physics, as we will see in the next section.

Going back to (46), we multiply (47) by v^μ , then using (52), we get for the last factor of (44),

$$\frac{1}{2M_B} \langle \bar{B} | \bar{b} b | \bar{B} \rangle = 1 - \frac{1}{2M^2} (\lambda_1 - 3\lambda_2) + \mathcal{O}\left(\frac{1}{M^3}\right), \quad (16.53)$$

where

$$\begin{aligned} \lambda_1 &= \frac{1}{2M_B} \langle \bar{B} | \bar{b} (\mathbf{iD})^2 b | \bar{B} \rangle, \quad (\mathbf{iD})^2 = (iv \cdot D)^2 - (\mathbf{iD})^2, \\ 3\lambda_2 &= \frac{1}{2M_B} \langle \bar{B} | \bar{b} \frac{g_s}{2} \sigma_{\mu\nu} G^{\mu\nu} b | \bar{B} \rangle. \end{aligned} \quad (16.54)$$

Equation (53) is remarkable in that the normalization (the term 1 on the right-hand side) is not only model-independent and unambiguously determined, but the $1/M$ correction is also absent because there is no dimensional $d = 4$ operators in (45).

Due to HQET, the spectator model receives a solid justification⁴. According to (44), (45), and (53), the decay width $\Gamma(\bar{B} \rightarrow X)$ is given by that of the free b quark decay $\Gamma(b \rightarrow X)$. Nonperturbative corrections due to bound-state effects start only at the $1/M^2$ order associated with the parameters λ_1 and λ_2 . Their physical meaning may be seen as follows. In the rest frame, the expectation value of the operator $(\mathbf{iD})^2$ is $\langle \mathbf{k}^2 \rangle$, i.e. λ_1 represents the spatial momentum of the b quark inside the \bar{B} . Its contribution is the field theory analog of the Lorentz contraction factor $\sqrt{1 - v_b^2} \approx 1 - (\mathbf{k}^2/2M^2)$ in accordance with the increase of the lifetime of a moving particle due to time dilatation. It cannot be computed by first principle, but only by some phenomenological analyses. We may estimate λ_1 to be $\simeq 0.3 \text{ GeV}^2$ using the mass formulas (30) and (31). As for λ_2 , from (32) we may take

$$\lambda_2 = \frac{1}{4} (M_{B^*}^2 - M_B^2) \approx 0.12 \text{ GeV}^2.$$

⁴ Bigi, I., Blok, B., Shifman, M., Uraltsev, N. and Vainshtein, A., in *B Decays* (ed. Stone, S.). World Scientific, Singapore 1994

16.3.2 Inclusive Semileptonic Decay: $\bar{B} \rightarrow e^- + \bar{\nu}_e + X_c$

Experiments indicate that the process $\bar{B} \rightarrow$ charmed hadrons dominates $\bar{B} \rightarrow$ unflavored hadrons, in particular the inclusive semileptonic decay $\bar{B} \rightarrow$ charm $+ e^- + \bar{\nu}_e$ largely exceeds $\bar{B} \rightarrow$ charmless $+ e^- + \bar{\nu}_e$. This implies $V_{cb} \gg V_{ub}$ for the CKM matrix.

As the first application of the general formalism just studied, we consider the dominant mode $\bar{B} \rightarrow e^- + \bar{\nu}_e + X_c$, where X_c represents the sum over all charmed hadrons. According to (44) and (53), the process is reliably described by $b \rightarrow c + e^- + \bar{\nu}_e$, and improved by corrections starting at $1/M^2$. This decay is important, it enables an accurate determination of V_{cb} and probes the dynamics of heavy flavors in the cleanest possible conditions, providing a testing ground for QCD to interplay quantitatively with weak interaction.

First, at the electroweak level uncorrected by QCD, $\Gamma(b \rightarrow c + \ell^- + \bar{\nu}_\ell)$ can be directly obtained from Chap. 13 where the rate of a fermion decaying into three fermions is given by (13.21), (13.62), or (13.63) accordingly. Thus,

$$\Gamma(b \rightarrow c + e^- + \bar{\nu}_e) = \frac{G_F^2 M^5}{192\pi^3} |V_{cb}|^2 f\left(\frac{m_c^2}{M^2}\right) \equiv \Gamma_0 |V_{cb}|^2 f\left(\frac{m_c^2}{M^2}\right), \quad (16.55)$$

with $f(x) = 1 - 8x + 8x^3 - x^4 - 12x^2 \log x$ taken from (13.22). We have neglected the electron and the neutrino masses. For the decay $b \rightarrow c + \tau^- + \bar{\nu}_\tau$ representing $\bar{B} \rightarrow \tau^- + \bar{\nu}_\tau + X_c$, the τ lepton mass cannot be neglected, the function $f(x)$ is replaced with the function $G(x, y)$ given by (13.62) where $x = m_c^2/M^2, y = m_\tau^2/M^2$.

Next we include QCD corrections to $b \rightarrow c + e^- + \bar{\nu}_e$ through the left vertex [bc] as shown in Fig. 16.3 and (5), so that (55) can be improved:

$$\Gamma(b \rightarrow c + e^- + \bar{\nu}_e) = \Gamma_0 |V_{cb}|^2 \left[f\left(\frac{m_c^2}{M^2}\right) - \frac{\alpha_s}{\pi} g\left(\frac{m_c^2}{M^2}\right) \right], \quad (16.56)$$

where $g(0) = \frac{2}{3} [\pi^2 - \frac{25}{4}] \approx 2.41$ is taken from (5).

The analytic expression of the function $g(x)$ is also known⁵, it decreases with increasing x , i.e. $g(x) < g(0)$. Nonperturbative bound-state effects (parameterized by λ_1 and λ_2) add new contributions to (56) and yield the rate $\Gamma(\bar{B} \rightarrow e^- + \bar{\nu}_e + X_c)$ following (44) and (53). Thus

$$\Gamma(\bar{B} \rightarrow e^- + \bar{\nu}_e + X_c) = \Gamma_0 \left\{ \left(1 - \frac{\lambda_1 - 3\lambda_2}{2M^2} \right) \left[f\left(\frac{m_c^2}{M^2}\right) - \frac{\alpha_s}{\pi} g\left(\frac{m_c^2}{M^2}\right) \right] - \frac{6\lambda_2}{M^2} \left(1 - \frac{m_c^2}{M^2} \right)^4 \right\} |V_{cb}|^2. \quad (16.57)$$

⁵ Nir, Y., Phys. Lett. **221B** (1989) 184; $g(x)$ is obtained by integrating over ξ the functions $R_u^v(\xi) + R_u^b(\xi)$ with $(\rho_2 = \rho_3 = 0)$ of Ho-Kim, Q. and Pham, Xuan-Yem, Phys. Lett. **122B** (1983) 297

The first nonperturbative term in (57) is the matrix element of the operator $\bar{b}b$ as given by (53), while the last term in (57) comes from the matrix element of the nonleading $1/M^2$ operator $g_s \bar{b} \sigma_{\mu\nu} G^{\mu\nu} b$ in (45). It is proportional to λ_2 defined in (54), accompanied by the phase space factor $(1-x)^4 = f(x) - \frac{1}{2} x \frac{df(x)}{dx}$ due to the nonzero c quark mass.

Equation (57) is important, since the width can be directly obtained using the semileptonic branching ratio $B(\bar{B} \rightarrow e^- + \bar{\nu}_e + X_c) \approx (10.9 \pm 0.46)\%$ together with the lifetime $\tau_B = (1.549 \pm 0.02) \times 10^{-12}$ s of the B meson: $\Gamma(\bar{B} \rightarrow e^- + \bar{\nu}_e + X_c) = B(\bar{B} \rightarrow e^- + \bar{\nu}_e + X_c)/\tau_B$. From these experimental data, the numerical value of the left-hand side of (57) is known. As for the right-hand side, using

$$M = (4.8 \pm 0.2) \text{ GeV} , \quad M - m_c = (3.4 \pm 0.06) \text{ GeV} , \quad (16.58)$$

one can extract the CKM matrix element $|V_{cb}|$ and find

$$|V_{cb}| = 0.04 \pm 0.004 . \quad (16.59)$$

The main uncertainty in (59) comes from the b quark mass M .

The magnitude of V_{ub} involving in $b \rightarrow u$ transition may be estimated by the electron energy spectrum in the decay $b \rightarrow q_1 + e^- + \bar{\nu}_e$ ($q_1 = c$ or u). Since the electron is emitted with either c or u quark, the electron spectrum is sensitive to the relative contributions of $b \rightarrow u + e^- + \bar{\nu}_e$ and $b \rightarrow c + e^- + \bar{\nu}_e$ and hence to the ratio V_{ub}/V_{cb} . Because the c is much heavier than the u quark, at high momentum transfer $q^2 > (M - m_c)^2$, or equivalently at high electron energy, only the $b \rightarrow u + e^- + \bar{\nu}_e$ contributes. Hence V_{ub} can be extracted at the so-called endpoint electron energy spectrum $E_e > M/2 = 2.4$ GeV, this region is populated only by the leptons in $b \rightarrow u + \ell^- + \bar{\nu}_\ell$. One gets $|V_{ub}/V_{cb}| \approx 0.08 \pm 0.02$. In the Wolfenstein version (11.79) of the CKM matrix, the value $|V_{ub}/V_{cb}| = \lambda \sqrt{\rho^2 + \eta^2} \approx 0.08 \pm 0.02$ in turn implies $\sqrt{\rho^2 + \eta^2} = 0.363 \pm 0.073$, using $\lambda = 0.2205 \pm 0.0018$. Also from (11.79), $|V_{cb}| = A \lambda^2$ and using (59), the parameter A can also be extracted. So,

$$A = 0.794 \pm 0.054 , \quad \sqrt{\rho^2 + \eta^2} = 0.363 \pm 0.073 . \quad (16.60)$$

16.3.3 Inclusive Nonleptonic Decay: $\bar{B} \rightarrow \text{Hadrons}$

This dominant mode (about 75% for the branching ratio) can be described by $b \rightarrow q_1 + q_2 + \bar{q}_3$ following the discussion after (45). There are eight combinations for the three quarks q_1 , q_2 , and \bar{q}_3 in the final state. They all contribute to the nonleptonic width and must be added up.

The decays $b \rightarrow c + d + \bar{u}$ and $b \rightarrow c + s + \bar{c}$ are dominant since favored by the CKM matrix elements $V_{cb}V_{ud}^*$ and $V_{cb}V_{cs}^*$ respectively, while the two others $b \rightarrow u + s + \bar{u}$ and $b \rightarrow u + d + \bar{c}$ are doubly suppressed by $V_{ub}V_{us}^*$ and

$V_{ub}V_{cd}^*$. The remaining modes $b \rightarrow c + s + \bar{u}$, $b \rightarrow c + d + \bar{c}$, $b \rightarrow u + d + \bar{u}$ and $b \rightarrow u + s + \bar{c}$ are moderately suppressed at the CKM level.

For definiteness, we consider the $b \rightarrow c + d + \bar{u}$ decay. The corresponding nonleptonic effective Lagrangian renormalized by QCD is given by (28):

$$\mathcal{L}_{\text{eff}} = \frac{G_F}{\sqrt{2}} V_{cb} V_{ud}^* [c_A \mathcal{O}_A + c_B \mathcal{O}_B] , \quad (16.61)$$

where \mathcal{O}_A is given by (3) and \mathcal{O}_B by (13) respectively, while

$$c_A = \frac{1}{2}[c_+(M) + c_-(M)] , \quad c_B = \frac{1}{2}[c_+(M) - c_-(M)] . \quad (16.62)$$

The coefficients $c_{\pm}(\mu)$ are given by (26). At the scale $\mu = M$, numerically we have $c_A \approx 1.12$ and $c_B \approx -0.28$.

The width $\Gamma(b \rightarrow c + d + \bar{u}) \sim |\langle c, d, \bar{u} | c_A \mathcal{O}_A + c_B \mathcal{O}_B | b \rangle|^2$ computed from the first term $c_A \mathcal{O}_A$ is familiar. We have met many times in \mathcal{O}_A the $(V - A) \times (V - A)$ currents involved in the decay of a fermion into three other fermions. The same remark applies to the second term $c_B \mathcal{O}_B$. The width obtained from these currents is given by $\Gamma_0 I(x, y, z)$ where $I(x, y, z)$ is taken⁶ from (13.63) or (13.66):

$$I(x, y, z) = 12 \int_{(x+y)^2}^{(1-z)^2} \frac{ds}{s} (s - x^2 - y^2)(1 + z^2 - s) [\lambda(s, x^2, y^2) \lambda(1, z^2, s)]^{1/2} ,$$

So the width – denoted by $\Gamma_{A^2 \oplus B^2}$ – coming from the direct contributions of \mathcal{O}_A and \mathcal{O}_B before their interference in $|\langle c, d, \bar{u} | c_A \mathcal{O}_A + c_B \mathcal{O}_B | b \rangle|^2$ is

$$\Gamma_{A^2 \oplus B^2} = \frac{G_F^2 M^5}{192\pi^3} |V_{cb} V_{ud}^*|^2 I \left(\frac{m_c}{M}, \frac{m_d}{M}, \frac{m_u}{M} \right) [c_A^2 + c_B^2] , \quad (16.63)$$

It remains to calculate the contribution to the width coming from the interference between the two operators \mathcal{O}_A and \mathcal{O}_B . Since the currents involved in these operators are different, it may be convenient to recast them in a form involving the same currents so that the interference can take place. For this purpose, let us rewrite \mathcal{O}_B as $\mathcal{O}_B \equiv (\bar{d}_e b_e) (\bar{c}_f u_f)$ where for simplification the $\gamma^\mu (1 - \gamma_5)$ is omitted in these two color-singlet currents $(\bar{d}b)$ and $(\bar{c}u)$. The color indices $e, f = 1, 2, 3$ are on the other hand explicitly written out, thus by Fierz rearrangement

$$\mathcal{O}_B = (\bar{d}_e b_e) (\bar{c}_f u_f) = (\bar{d}_e u_f) (\bar{c}_f b_e) .$$

The last term on the right-hand side of the above equation can be cast into a form close to \mathcal{O}_A in order to interfere with it. With (11.88) or (11) we get

$$(\bar{d}_e u_f) (\bar{c}_f b_e) = \frac{1}{3} (\bar{d}_e u_e) (\bar{c}_f b_f) + 2 \sum_j [\bar{d}_e (T^j)_{ef} u_f] [\bar{c}_g (T^j)_{gh} b_h]$$

⁶ Cortes, J. L., Pham, X. Y. and Tounsi, A. Phys. Rev. **D25** (1982) 188

which immediately gives

$$\mathcal{O}_B = \frac{1}{3}\mathcal{O}_A + 2 \sum_{j=1}^8 [\bar{d} T^j u] [\bar{c} T^j b]. \quad (16.64)$$

Similarly, we also have

$$\mathcal{O}_A = \frac{1}{3}\mathcal{O}_B + 2 \sum_{j=1}^8 [\bar{d} T^j b] [\bar{c} T^j u]. \quad (16.65)$$

From (64), we see that in \mathcal{O}_B only the operator $\frac{1}{3}\mathcal{O}_A$ can be used to interfere with \mathcal{O}_A . The color-octet currents $\bar{d} T^j u$ and $\bar{c} T^j b$ cannot interfere with the color-singlet currents in \mathcal{O}_A . The contribution to the $b \rightarrow c + d + \bar{u}$ rate due to the interference between the two operators $c_A \mathcal{O}_A$ and $c_B \mathcal{O}_B$ in $|c_A \mathcal{O}_A + c_B \mathcal{O}_B|^2$ must come only from \mathcal{O}_A or \mathcal{O}_B . Thus,

$$|(c_A + \frac{1}{3}c_B)\mathcal{O}_A|^2, \text{ or } |(\frac{1}{3}c_A + c_B)\mathcal{O}_B|^2 \xrightarrow{\text{interference}} \frac{2}{3}c_A c_B |\mathcal{O}_A|^2, \text{ or } \frac{2}{3}c_A c_B |\mathcal{O}_B|^2$$

which gives

$$\Gamma_{A \otimes B} = \frac{G_F^2 M^5}{192\pi^3} |V_{cb} V_{ud}^*|^2 I \left(\frac{m_c}{M}, \frac{m_d}{M}, \frac{m_u}{M} \right) \left[\frac{2}{3} c_A c_B \right]. \quad (16.66)$$

Adding (63) to (66), with $c_A^2 + c_B^2 + \frac{2}{3}c_A c_B = \frac{1}{3}(2c_+^2 + c_-^2)$, the $b \rightarrow c + d + \bar{u}$ rate derived from the effective Lagrangian (61) is

$$\Gamma(b \rightarrow c + d + \bar{u}) = \frac{G_F^2 M^5}{192\pi^3} |V_{cb} V_{ud}^*|^2 I \left(\frac{m_c}{M}, \frac{m_d}{M}, \frac{m_u}{M} \right) \left[\frac{2c_+^2 + c_-^2}{3} \right]. \quad (16.67)$$

A direct calculation of the width from (61) without passing by (64) is tedious, and of course one should recover (67). This general formula can be used for all $\Gamma(b \rightarrow q_1 + q_2 + \bar{q}_3)$ with the appropriate changes in $\Gamma_0 |V_{bq_1} V_{q_2 q_3}^*|^2 I(m_{q_1}/M, m_{q_2}/M, m_{q_3}/M)$ symbolically denoted by $\tilde{\Gamma}_0$.

The factor $(2c_+^2 + c_-^2)$, which is the *leading logarithmic* correction to the decay rate, represents the summation $|\sum_n (\alpha_s \log M/\mu)^n|^2$ by the renormalization group equation. The nonleading α_s QCD corrections to the rate as given by (6) could also be added for completeness. For the decay $b \rightarrow c + d + \bar{u}$, this nonleading correction to be added to (67) is $[-1.41 \alpha_s/\pi] \times \tilde{\Gamma}_0$ if we neglect the three final quark masses. As discussed after (6), for $m_c = 0.3 M$ and $m_u = m_d = 0$, the correction is in fact $[-0.35 \alpha_s/\pi] \times \tilde{\Gamma}_0$ which is small. However, for the decay $b \rightarrow c + s + \bar{c}$, this α_s correction is especially important because of the massive $s + \bar{c}$ quarks at the right vertex as discussed previously (Fig. 16.4). Instead of $[-0.35 \alpha_s/\pi] \times \tilde{\Gamma}_0$, one has $[+3.02 \alpha_s/\pi] \times \tilde{\Gamma}_0$ which enhances the $b \rightarrow c + s + \bar{c}$ rate.

To get the inclusive nonleptonic decay rate of \bar{B} into charmed hadrons, denoted by $\Gamma(\bar{B} \rightarrow X_c)$, from $\Gamma(b \rightarrow c + d + \bar{u})$ as given by (67), the color factor $N_c = 3$ must be included by summing over the colors of the pair $d + \bar{u}$. This is to be compared with the inclusive semileptonic rate $\Gamma(b \rightarrow c + \ell^- + \bar{\nu}_\ell)$ in (55) where the quark pair $d + \bar{u}$ replaces the lepton pair $\ell^- + \bar{\nu}_\ell$. Neglecting the u and d masses and the nonleading α_s corrections, we have from (67) and $f(x) = I(x, 0, 0)$

$$\Gamma(\bar{B} \rightarrow X_c) = [2c_+^2 + c_-^2] |V_{cb}V_{ud}^*|^2 f\left(\frac{m_c^2}{M^2}\right) \Gamma_0. \quad (16.68)$$

Since $2c_+^2 + c_-^2 > 3$, the leading logarithm QCD renormalization effect *always enhances* the hadronic rate. It is gratifying to recover the old formula when the pure electroweak Lagrangian is not renormalized by QCD, i.e. with $\alpha_s = 0$, $c_A = 1$, and $c_B = 0$ ($c_+ = c_- = 1$), thus

$$[2c_+^2 + c_-^2] \longrightarrow 3, \text{ and } \Gamma(\bar{B} \rightarrow X_c) \longrightarrow 3 |V_{cb}V_{ud}^*|^2 f\left(\frac{m_c^2}{M^2}\right) \Gamma_0, \quad (16.69)$$

which is three times the inclusive semileptonic rate $\Gamma(\bar{B} \rightarrow X_c + e^- + \bar{\nu}_e)$ naively expected from counting the color number $N_c = 3$.

Finally, the nonperturbative b quark effect inside the B meson can be appropriately improved by the factor $[1 - (\lambda_1 - 3\lambda_2)/(2M^2)]$ corresponding to the leading term of the $\bar{b}b$ operator, as in (57). We have

$$\Gamma(\bar{B} \rightarrow X_c) = [2c_+^2 + c_-^2] |V_{cb}V_{ud}^*|^2 f\left(\frac{m_c^2}{M^2}\right) \left[1 - \frac{\lambda_1 - 3\lambda_2}{2M^2}\right] \Gamma_0. \quad (16.70)$$

The inclusive nonleptonic rate is an important quantity contributing to the total lifetime, from which various branching ratios (in particular the semileptonic branching ratio) can be derived.

16.4 Exclusive Decays

Being complementary to the inclusive decays, the exclusive modes are extensively investigated on both experimental and theoretical sides. Exclusive decays are particularly important for testing the dynamics of heavy flavors. The form factors involved in the bottom decaying into charm can be determined within the framework of HFS, since both b and c are heavy. Actually the most precise determination of the CKM matrix element V_{cb} comes from the exclusive mode $\bar{B} \rightarrow D^* + e^- + \bar{\nu}_e$. We first study the semileptonic decays, then discuss the two-body hadronic modes using the factorization method, which turns out to be a good approximation, as we will see.

16.4.1 Form Factors in $B_{\ell 3}$ Decays

There are several reasons for the semileptonic decays to play a prominent role in heavy flavor B physics. These decays are the simplest to understand theoretically through the spectator diagram shown in Fig. 16.7. Only the form factors are unknown, but they can be reliably determined from HFS. Secondly, the charge of the detected lepton identifies the flavor of the B hadron according to the $\Delta B = \Delta Q$ rule similar to the $\Delta S = \Delta Q$, i.e. an emitted negative lepton charge shows that a \bar{B} meson is involved, and conversely a positive lepton charge represents a B meson. Thirdly, semileptonic branching ratios are large in B decays, allowing for extensive experimental investigations. These modes are used to measure the CKM matrix elements V_{cb} and V_{ub} , and the size of the B^0 – \bar{B}^0 mixing.

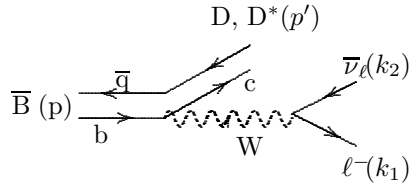


Fig. 16.7. $\bar{B} \rightarrow D (D^*) + \ell^- + \bar{\nu}_\ell$

Like the $K_{\ell 3}$, the simplest $B_{\ell 3}$ decay is $\bar{B}(p) \rightarrow D(p') + \ell^-(k_1) + \bar{\nu}_\ell(k_2)$. Its amplitude can be written as a product of the $\bar{B} \rightarrow D$ transition induced by the hadronic vector current $V^\mu = \bar{c}\gamma^\mu b$ times the leptonic current

$$\mathcal{A} = \frac{G_F V_{cb}}{\sqrt{2}} \langle D(p') | V^\mu | \bar{B}(p) \rangle \bar{u}(k_1) \gamma_\mu (1 - \gamma_5) v(k_2). \quad (16.71)$$

As explained in Sect. 10.1, the matrix element of any axial current (in particular $A^\mu = \bar{c}\gamma^\mu \gamma_5 b$) between the two pseudoscalar mesons must vanish, hence only V^μ contributes. As discussed in (10.15), on general grounds, the $\langle D(p') | V^\mu | \bar{B}(p) \rangle$ matrix element is expressed in terms of the two form factors $f_\pm(q^2)$, with $q^\mu = (p - p')^\mu$:

$$\langle D(p') | V^\mu | \bar{B}(p) \rangle = f_+(q^2) (p + p')^\mu + f_-(q^2) (p - p')^\mu. \quad (16.72)$$

The heavy flavor symmetry (between the b and c quarks) enables us to determine the normalizations of the form factors at $q_{\max}^2 = (M_B - M_D)^2$. Starting from (47) we make use of the flavor symmetry to replace the b quark in the final state meson by the c quark, thereby turning B meson into D meson. Then (47) becomes

$$\frac{1}{\sqrt{M_B M_D}} \langle D(v') | \bar{c}\gamma^\mu b | \bar{B}(v) \rangle = \xi(v \cdot v') (v + v')^\mu \quad (16.73)$$

where the same Isgur–Wise function $\xi(\omega)$ is involved. Comparing (72) with (73), we obtain

$$f_{\pm}(q^2) = \frac{M_D \pm M_B}{2\sqrt{M_B M_D}} \xi(v \cdot v') . \quad (16.74)$$

Thus HFS relates two independent form factors $f_{\pm}(q^2)$ to the same function $\xi(v \cdot v')$. Most importantly, with (52), the normalization $\xi(v \cdot v' = 1) = 1$ implies a nontrivial normalization of the form factors $f_{\pm}(q^2)$ at the maximum momentum transfer q_{\max}^2 . Since $q^2 = M_B^2 + M_D^2 - 2 M_B M_D v \cdot v'$, the zero-recoil limit $\omega = 1$ is equivalent to $q_{\max}^2 = (M_B - M_D)^2$, thus

$$f_{\pm}(q_{\max}^2) = \frac{M_D \pm M_B}{2\sqrt{M_B M_D}} \quad (16.75)$$

as already announced in (10.16). This model-independent result is valid in the limit of heavy b and c masses much larger than $\Lambda_{\text{QCD}} \simeq 0.2\text{GeV}$.

The transition between the pseudoscalar $\bar{B}(p)$ and the vector $D^*(p', \epsilon)$ mesons depends on four independent form factors⁷, one with $V_{cb}^{\mu} = \bar{c}\gamma^{\mu} b$ and three with $A_{cb}^{\mu} = \bar{c}\gamma^{\mu}\gamma_5 b$. They are

$$\begin{aligned} \langle D^*(p', \epsilon) | \bar{c}\gamma^{\mu} b | \bar{B}(p) \rangle &= 2i \epsilon^{\mu\nu\alpha\beta} \frac{\epsilon_{\nu} p'_{\alpha} p_{\beta}}{M_B + M_{D^*}} V(q^2) , \\ \langle D^*(p', \epsilon) | \bar{c}\gamma^{\mu} \gamma_5 b | \bar{B}(p) \rangle &= (M_B + M_{D^*}) \left[\epsilon^{\mu} - \frac{\epsilon \cdot q q^{\mu}}{q^2} \right] A_1(q^2) \\ &\quad - \epsilon \cdot q \left[\frac{(p + p')^{\mu}}{M_B + M_{D^*}} - \frac{(M_B - M_{D^*}) q^{\mu}}{q^2} \right] A_2(q^2) \\ &\quad + 2M_{D^*} \frac{\epsilon \cdot q q^{\mu}}{q^2} A_0(q^2) . \end{aligned} \quad (16.76)$$

In the above equations, the three tensors associated with $V(q^2)$, $A_1(q^2)$, and $A_2(q^2)$ are constructed to be orthogonal to $q_{\mu} = (p - p')_{\mu}$ such that they vanish when multiplied by $q_{\mu} = (p - p')_{\mu}$. The linear combination

$$A_3(q^2) \equiv \frac{M_B + M_{D^*}}{2M_{D^*}} A_1(q^2) - \frac{M_B - M_{D^*}}{2M_{D^*}} A_2(q^2) \quad (16.77)$$

is subject to the constraint $A_3(0) = A_0(0)$ so that no pole occurs at $q^2 = 0$.

The spin symmetry leads to additional relations among these four form factors. Using this symmetry, the vector meson D^* with longitudinal polarization ϵ_3 is related to the D meson by

$$|D^*(v', \epsilon_3)\rangle = 2\mathbf{S}_3 |D(v')\rangle , \quad (16.78)$$

⁷ Wirbel, M., Stech, B. and Bauer, M., Z. Phys. **C29** (1985) 637

where \mathbf{S}_3 is a Hermitian operator acting on the c quark, its matrix representation is denoted by S_3 . In a general frame, one can define a set of three orthonormal vectors ϵ_i orthogonal to v^i from which the generators of the spin symmetry may be taken as

$$\mathbf{S}_i = \frac{1}{2} \gamma_5 \not{v} \not{\epsilon}_i .$$

From (78), it follows that

$$\langle D^*(v', \epsilon_3) | \gamma^\mu (1 - \gamma_5) | \bar{B}(v) \rangle = \langle D(v') | 2 [\mathbf{S}_3, \gamma^\mu (1 - \gamma_5)] | \bar{B}(v) \rangle . \quad (16.79)$$

For the evaluation of the above commutators, it is convenient to use the rest frame of the final state D^* meson

$$v'^\mu = (1, 0, 0, 0) , \quad \epsilon_3^\mu = (0, 0, 0, 1) , \quad \mathbf{S}_3 = \frac{1}{2} \gamma_5 \gamma^0 \gamma_3 ,$$

and get

$$\begin{aligned} 2 [\mathbf{S}_3, \gamma^0 (1 - \gamma_5)] &= -\gamma^3 (1 - \gamma_5) , \quad 2 [\mathbf{S}_3, \gamma^3 (1 - \gamma_5)] = -\gamma^0 (1 - \gamma_5) , \\ 2 [\mathbf{S}_3, \gamma^1 (1 - \gamma_5)] &= -i\gamma^2 (1 - \gamma_5) , \quad 2 [\mathbf{S}_3, \gamma^2 (1 - \gamma_5)] = +i\gamma^1 (1 - \gamma_5) . \end{aligned}$$

From (79) and the above equation, one can obtain the matrix element of the $\bar{B}(v) \rightarrow D^*(v')$ transition from the $\bar{B}(v) \rightarrow D(v')$ transition, both are related to the universal function $\xi(v \cdot v')$:

$$\begin{aligned} \frac{1}{\sqrt{M_B M_{D^*}}} \langle D^*(v', \epsilon_3) | \bar{c} \gamma^\mu \gamma_5 b | \bar{B}(v) \rangle &= [(1 + \omega) \epsilon^\mu - (\epsilon \cdot v) v'^\mu] \xi(v \cdot v') , \\ \frac{1}{\sqrt{M_B M_{D^*}}} \langle D^*(v', \epsilon_3) | \bar{c} \gamma^\mu b | \bar{B}(v) \rangle &= i \epsilon^{\mu\nu\alpha\beta} \epsilon_\nu v'_\alpha v_\beta \xi(v \cdot v') . \end{aligned} \quad (16.80)$$

Comparing (80) with (76), the four form factors are now related to $\xi(\omega)$ by

$$\begin{aligned} \frac{M_B + M_{D^*}}{2\sqrt{M_B M_{D^*}}} \xi(\omega) &= V(q^2) = A_2(q^2) = A_0(q^2) \\ &= \left[1 - \frac{q^2}{(M_B + M_{D^*})^2} \right]^{-1} A_1(q^2) . \end{aligned} \quad (16.81)$$

At $q_{\max}^2 = (M_B - M_{D^*})^2$ for which $\omega = 1$, their normalizations are

$$\frac{(M_B + M_{D^*})^2}{4 M_B M_{D^*}} A_1(q_{\max}^2) = V(q_{\max}^2) = A_2(q_{\max}^2) = A_0(q_{\max}^2) = \frac{M_B + M_{D^*}}{2\sqrt{M_B M_{D^*}}} .$$

This remarkable relation is a model-independent result, like (75). The six independent form factors in (72) and (76) are expressed in terms of the universal $\xi(\omega)$ function, normalized by $\xi(1) = 1$. On the other hand, the q^2 behavior of the form factors as well as the ω dependence of $\xi(\omega)$ are not determined by the heavy flavor symmetry.

16.4.2 Semileptonic Decay Rates

Equipped with these form factors we are now ready to compute the $B_{\ell 3}$ decay rates. From the amplitude of $\bar{B}(p) \rightarrow D(p') + \ell^-(k_1) + \bar{\nu}_\ell(k_2)$ in (71), the rate is given according to the general formulas (4.55) and (4.70) by

$$d\Gamma = \frac{1}{2M_B(2\pi)^5} \frac{d^3p'}{2E'} \frac{d^3k_1}{2E_1} \frac{d^3k_2}{2E_2} \sum_{\text{spins}} |\mathcal{A}|^2 \delta^4(q - k_1 - k_2), \quad (16.82)$$

where $q = p - p'$. Using (74), we have

$$\mathcal{A} = \frac{G_F V_{cb}}{\sqrt{2}} \frac{M_B + M_D}{\sqrt{M_B M_D}} \xi(\omega) \left\{ \bar{u}(k_1) \not{p}' (1 - \gamma_5) v(k_2) - \frac{m_\ell M_B}{M_B + M_D} \bar{u}(k_1) (1 - \gamma_5) v(k_2) \right\}; \quad (16.83)$$

the last term proportional to the lepton mass m_ℓ may be neglected for electron or muon, in which case

$$\sum_{\text{spins}} |\mathcal{A}|^2 = \left\{ 16 G_F^2 |V_{cb}|^2 |f_+(q^2)|^2 \right\} \left[2(p \cdot k_1)(p \cdot k_2) - M_B^2(k_1 \cdot k_2) \right].$$

In the rest frame of the decaying \bar{B} , $q^2 = M_B^2 + M_D^2 - 2M_B E'$, we have

$$\frac{d^3p'}{2E'} = 2\pi |\mathbf{p}'| dE' \quad , \quad |\mathbf{p}'| = \frac{\sqrt{\lambda(M_B^2, M_D^2, q^2)}}{2M_B} = M_D \sqrt{\omega^2 - 1} \quad , \quad E' = \omega M_D.$$

Thus

$$d\Gamma = \frac{2\pi |\mathbf{p}'| dE'}{2M_B(2\pi)^5} \left\{ 16 G_F^2 |V_{cb}|^2 |f_+(q^2)|^2 \right\} \left[2p_\mu p_\nu - g_{\mu\nu} M_B^2 \right] I^{\mu\nu}, \quad (16.84)$$

where $I^{\mu\nu}$ is the phase space integration of the lepton pair $\sim \int d^3k_1 d^3k_2$ already given by (13.11). Since the neutrino is unobserved, we integrate first (82) over its momentum $\int d^3k_2$ to obtain the double distributions of the charged lepton energy E_ℓ and the D meson energy E' , the E' distribution is equivalent to the q^2 distribution, since $dq^2 = 2M_B dE'$:

$$\frac{d\Gamma}{dq^2 dE_\ell} = \frac{G_F^2 |V_{cb}|^2}{16\pi^3} |f_+(q^2)|^2 \left\{ 2(M_B^2 - M_D^2 + q^2) \frac{E_\ell}{M_B} - 4E_\ell^2 - q^2 \right\}.$$

To obtain the q^2 distribution, instead of integrating the above equation over E_ℓ , we take directly (84) and use

$$\left[2p_\mu p_\nu - g_{\mu\nu} M_B^2 \right] I^{\mu\nu} = \frac{\pi}{24} \lambda(M_B^2, M_D^2, q^2) \equiv \frac{\pi}{6} M_B^2 |\mathbf{p}'|^2. \quad (16.85)$$

Putting (85) into (84), the result is

$$\begin{aligned} \frac{d\Gamma(\bar{B} \rightarrow D + e^- + \bar{\nu}_e)}{dq^2} &= \frac{G_F^2 |V_{cb}|^2}{24 \pi^3} |\mathbf{p}'|^3 |f_+(q^2)|^2, \\ \text{or } \frac{d\Gamma}{d\omega} &= \frac{G_F^2 |V_{cb}|^2}{48 \pi^3} (M_B + M_D)^2 M_D^3 \left(\sqrt{\omega^2 - 1} \right)^3 \xi^2(\omega), \\ m_\ell^2 \leq q^2 &\leq (M_B - M_D)^2, \quad 1 \leq \omega \leq \frac{M_B^2 + M_D^2 - m_\ell^2}{2 M_B M_D}. \end{aligned} \quad (16.86)$$

For $\bar{B} \rightarrow D + \tau^- + \bar{\nu}_\tau$, the tau lepton mass m_ℓ cannot be neglected, then

$$\frac{d\Gamma}{dq^2} = \frac{G_F^2 |V_{cb}|^2}{24 \pi^3} |\mathbf{p}'|^3 (1 - 2\rho)^2 \left\{ (1 + \rho) |f_+(q^2)|^2 + 3\rho |f_0(q^2)|^2 \right\}, \quad (16.87)$$

where

$$\rho = \frac{m_\ell^2}{2q^2} \quad \text{and} \quad f_0(q^2) = \frac{(M_B^2 - M_D^2)f_+(q^2) + q^2 f_-(q^2)}{2M_B |\mathbf{p}'|}. \quad (16.88)$$

The distribution (86) determines the q^2 dependence of the form factor $f_+(q^2)$, specially the ω dependence of the universal function $\xi(\omega)$. Furthermore, taking advantage of the normalization $\xi(1) = 1$, the only unknown in (86) is V_{cb} , therefore once the kinematic term $(\sqrt{\omega^2 - 1})^3$ is subtracted from the differential rate $d\Gamma/d\omega$, its value at $\omega \rightarrow 1$ determines $|V_{cb}|$.

In fact, this method is used to study the process $\bar{B} \rightarrow D^* + e^- + \bar{\nu}_e$ which has the largest branching ratio. Furthermore, with the vector meson D^* , measurements of its helicity amplitudes by the angular distributions provide a detailed study of the form factors $V(q^2)$, $A_1(q^2)$, and $A_2(q^2)$, and the relation (81) can be checked. The longitudinal H_0 and transverse H_\pm helicity amplitudes of the D^* are related to the form factors by

$$\begin{aligned} H_0(q^2) &= \frac{M_B + M_{D^*}}{2M_{D^*} \sqrt{q^2}} \left[(M_B^2 - M_{D^*}^2 - q^2) A_1(q^2) - \frac{4M_B^2 |\mathbf{p}'|^2}{(M_B + M_{D^*})^2} A_2(q^2) \right], \\ H_\pm(q^2) &= (M_B + M_{D^*}) \left[A_1(q^2) \mp \frac{2M_B |\mathbf{p}'|}{(M_B + M_{D^*})^2} V(q^2) \right]. \end{aligned} \quad (16.89)$$

There are three angular distributions that could be used to separate the helicity amplitudes: the angle of the π^+ in the rest frame of the D^* which decays into $D + \pi$, the e^- angle in the lepton pair rest frame and the correlation between these two decay planes. The q^2 distribution is found to be

$$\frac{d\Gamma(\bar{B} \rightarrow D^* + e^- + \bar{\nu}_e)}{dq^2} = \frac{G_F^2 |V_{cb}|^2}{96 \pi^3} \frac{q^2 |\mathbf{p}'|}{M_B^2} \sum_{i=0,\pm} |H_i(q^2)|^2. \quad (16.90)$$

Using (81), (89), and (90), one gets

$$\begin{aligned} \frac{d\Gamma(\bar{B} \rightarrow D^* + e^- + \bar{\nu}_e)}{d\omega} &= \frac{G_F^2 |V_{cb}|^2}{48 \pi^3} (M_B - M_{D^*})^2 M_{D^*}^3 \sqrt{\omega^2 - 1} (\omega + 1)^2 \\ &\times \left[1 + \frac{4\omega}{\omega + 1} \frac{q^2(\omega)}{(M_B - M_{D^*})^2} \right] \xi^2(\omega), \end{aligned} \quad (16.91)$$

where $q^2(\omega) = M_B^2 + M_{D^*}^2 - 2\omega M_{D^*} M_B$.

In principle (91) should be corrected for the fact that the heavy quarks are not infinitely large. Fortunately, there exists a theorem⁸ which states that at $\omega = 1$, the leading $1/M$ correction vanishes, such that only corrections of order $1/M^2$ are needed for the modes with a vector meson in the final state, e.g. the D^* considered here.

Once the kinematic terms in (91) are subtracted from the $d\Gamma/d\omega$ distribution, the value of the latter at $\omega = 1$ allows the determination of V_{cb} by taking advantage of $\xi(1) = 1 + \mathcal{O}(1/M^2)$. One gets⁹

$$|V_{cb}| = 0.039 \pm 0.003, \quad (16.92)$$

which is in remarkable agreement with the inclusive semileptonic decay (59).

16.4.3 Two-Body Hadronic Decays

Nonleptonic decays of B mesons have been extensively observed and hundreds of channels have been identified, most of them being the two-body modes like $\bar{B} \rightarrow D + \pi$, or quasi-two-body like $\bar{B} \rightarrow \bar{K}^* + \psi$. Above all, the studies of nonleptonic decays must deal with the *matrix element* of the operator product $H^\mu H_\mu^\dagger$ inserted between the decaying parent hadron \mathcal{P} and the hadrons in the final state collectively denoted by \mathcal{F} . This is in contrast to the semileptonic decay modes $\mathcal{P} \rightarrow \mathcal{F} + \bar{\ell} + \nu_\ell$ for which only the single operator H^μ enters and the decay amplitude is a product of the well-determined matrix element of the leptonic current $\langle \bar{\ell} + \nu_\ell | L_\mu^\dagger | 0 \rangle = \bar{u}_\nu \gamma_\mu (1 - \gamma_5) v_\ell$ times the matrix element $\langle \mathcal{F} | H^\mu | \mathcal{P} \rangle$. The latter is expressed in terms of form factors which are theoretically more or less tractable, and experimentally measurable. This property for an amplitude to be equal to the product of the matrix elements of separate currents is called the *factorization* property.

Factorization. The factorization ansatz for nonleptonic decays is inspired by the semileptonic decay amplitudes which are always factorized into a product of two matrix elements, that of the quark current H^μ and the lepton current L_μ . Quarks and leptons are separated by the W boson propagator, and gluons cannot connect them; a typical example is (71).

⁸ Luke, M. E., Phys. Lett. **252B** (1990) 447; analog of the Ademollo–Gatto theorem in Phys. Rev. Lett. **13** (1964) 264

⁹ Stone, S., in B Decays, World Scientific, Singapore 1994; Neubert, M., Int. J. Mod. Phys. **A11** (1996) 4173

This is not the case of nonleptonic decays, generically described by $Q \rightarrow q_1 + q_2 + \bar{q}_3$, where soft gluons exchanged among quarks of the two currents $H_{Qq_1}^\mu = \bar{q}_1 \gamma^\mu (1 - \gamma_5) Q$ and $H_{q_2 q_3}^\mu = \bar{q}_2 \gamma^\mu (1 - \gamma_5) q_3$ make factorization *a priori* inapplicable. For the hadronic decays $\mathcal{P} \rightarrow \mathcal{F}$, the matrix element $\langle \mathcal{F} | H^\mu H_\mu^\dagger | \mathcal{P} \rangle$ is involved; if we insert hadronic intermediate states between the product $H^\mu H_\mu^\dagger$, we would not know how many states to include.

However, for the two-body decays of a heavy particle, there is a physical reason supporting factorization; it may be understood through the intuitive¹⁰ ‘color transparency argument’. Because of the large mass of the decaying particle in energetic two-body transitions, hadronization by soft gluons exchanged among the decay products does not occur until they have traveled some distance away from each other. The reason is that once the two color-singlet quarks are formed in H^μ and H_μ^\dagger separately, soft gluons are ineffective in rearranging them. Created in a pointlike interaction $b \rightarrow c + d + \bar{u}$, a fast-moving colorless $\bar{u}d$ quark pair leaves the interaction region in the same direction with a velocity close to the speed of light and will hadronize only after a time given by its $\gamma = [\sqrt{1 - (v^2/c^2)}]^{-1}$ factor multiplied by a typical hadronization time $\tau_{\text{had}} \sim 1 \text{ fm}/c$. In this example, this means that hadronization occurs about 20 fm away from the remaining $c + \bar{q}$ quarks (\bar{q} being the spectator light constituent of the \bar{B} meson). Inside the weak interaction region, the $\bar{u}d$ colorless pair behaves like a hadron and does not interact with the remaining colorless $c\bar{q}$ pair which forms the second hadron.

The factorization is a working hypothesis which turns out to be a good approximation and can be tested, at least for a class of two-body reactions. Using factorization, nonleptonic two-body decays are not only the cleanest channels to study but also provide an instrument for exploring the most interesting aspect of nonperturbative QCD. Indeed, since the decaying heavy particle can be isolated and the weak transition has a well-determined structure, a detailed analysis of the decay products with different spin and flavor provides precious information about the long-range forces that govern the internal structure of hadrons. Especially interesting are the form factors and the decay constants, which describe the quark–antiquark attraction inside a hadron. As many of them are not experimentally accessible in leptonic or electromagnetic processes, nonleptonic decays provide a way to extract them.

To illustrate the factorization method, we consider the two-body modes $\bar{B} \rightarrow D + \pi$, $\bar{B} \rightarrow D^* + \pi$, and $\bar{B} \rightarrow D + \rho$ for both charged and neutral decaying \bar{B} meson. The corresponding Lagrangian which governs these decays are given by (61) and (62). The mesons in the final state can be directly generated by the quark current carrying the appropriate flavor quantum numbers. The three quarks c , d , and \bar{u} in the final state then combine with the light \bar{q} constituent of the \bar{B} meson to form the charmed and unflavored hadrons in the decay products, for instance $\bar{B} \rightarrow D + \pi$. There are essentially two ways for the spectator \bar{q} to combine with the other three quarks c , d , and \bar{u} to

¹⁰ Bjorken, J. D., Nucl. Phys. (Proc. Suppl.) **B11** (1989) 325

generate D and π . Either D comes from the combination $c+\bar{q}$ and π from $d+\bar{u}$ (Fig. 16.8a), or D comes from $c+\bar{u}$, and π from the other combination $d+\bar{q}$ (Fig. 16.8b). The latter is sometimes called the color-suppressed mode, for a reason that will be clear soon.

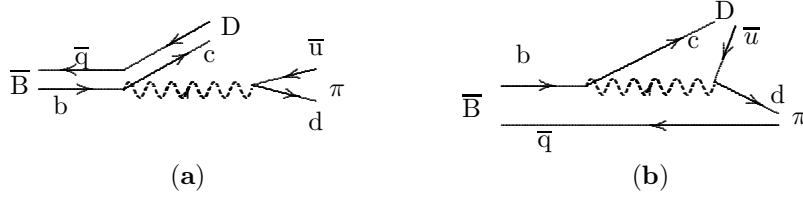


Fig. 16.8. Spectator picture for (a) $\bar{B}^0 \rightarrow D^+ + \pi^-$, and (b) $\bar{B}^0 \rightarrow D^0 + \pi^0$, the light constituent $\bar{q} = \bar{d}$ of \bar{B}^0 is spectator

Thus, like the semileptonic formula (71) and Fig. 16.7, the amplitude factorizes into the product of the matrix elements of two color-singlet quark currents. For instance, the amplitude of $\bar{B}^0(p) \rightarrow D^+(p') + \pi^-(q)$ in Fig. 16.8a may be written as

$$\mathcal{M}_{\pi^- D^+} = a_1 \frac{G_F}{\sqrt{2}} V_{cb} V_{ud}^* \langle \pi^-(q) | \bar{d} \gamma_\mu \gamma_5 u | 0 \rangle \langle D^+(p') | \bar{c} \gamma^\mu b | \bar{B}^0(p) \rangle, \quad (16.93)$$

where the coefficient a_1 is defined as follows: we go back to (61), (62), and especially using (64), to write the nonleptonic effective Lagrangian as

$$\begin{aligned} \mathcal{L}_{\text{eff}} &= \frac{G_F}{\sqrt{2}} V_{cb} V_{ud}^* \left\{ \left(c_A + \frac{1}{N_c} c_B \right) \mathcal{O}_A + 2c_B \sum_j [\bar{d} T^j u] [\bar{c} T^j b] \right\} \\ &= \frac{G_F}{\sqrt{2}} V_{cb} V_{ud}^* [a_1 \mathcal{O}_A + \dots], \quad \text{where } a_1 = c_A + \frac{1}{N_c} c_B, \end{aligned} \quad (16.94)$$

the dots represent the second term with color-non-singlets T^j currents.

Unlike (93), the matrix element of the second operator vanishes when we insert colorless hadrons between $T^j \cdot T^j$, e.g. $\langle \pi | \bar{d} T^j u | 0 \rangle \times \langle D | \bar{c} T^j b | B \rangle = 0$. Whereas for \mathcal{O}_A , which is the product $[\bar{c} \gamma_\mu (1 - \gamma_5) b] \times [\bar{d} \gamma^\mu (1 - \gamma_5) u]$ of two color-singlet currents, the insertion of hadronic states (or vacuum) between these currents yields nonzero result as explicitly shown by (93). The $\langle D\pi | \bar{d} T^j u \bar{c} T^j b | B \rangle$ term which constitutes the nonfactorizable contribution is discarded.

Since everything in (93) is known,

$$\begin{aligned} \langle \pi^-(q) | \bar{d} \gamma_\mu \gamma_5 u | 0 \rangle &= i f_\pi q_\mu = i f_\pi (p - p')_\mu, \\ \langle D^+(p') | \bar{c} \gamma^\mu b | \bar{B}^0(p) \rangle &= (p + p')^\mu f_+(q^2) + q^\mu f_-(q^2), \end{aligned}$$

we obtain

$$\mathcal{M}_{\pi^- D^+} = i a_1 \frac{G_F}{\sqrt{2}} V_{cb} V_{ud}^* f_\pi [(M_B^2 - M_D^2) f_+(m_\pi^2) + m_\pi^2 f_-(m_\pi^2)] , \quad (16.95)$$

where $f_\pm(q^2)$ are given in (74); the last term $\sim m_\pi^2$ may be neglected.

The process $\bar{B}^0 \rightarrow D^+ + \pi^-$ associated with $a_1 \mathcal{O}_A$ of (94) is shown in Fig. 16.8a. This $\bar{B}^0 \rightarrow D^+ + \pi^-$ decay is similar to the semileptonic mode $\bar{B}^0 \rightarrow D^+ + \ell^- + \bar{\nu}_\ell$ shown in Fig. 16.7 with the π^- replacing the $\ell^- + \bar{\nu}_\ell$ pair. Let us call class I the modes governed by the $a_1 \mathcal{O}_A$ operator. All decay modes $\bar{B}^0 \rightarrow H_c^+ + h^-$ where H_c^+ are charmed mesons (D^+ , D^{*+} etc.) and h^- unflavored mesons (π^- , ρ^- , $a_1^-(1260)$, etc.) belong to class I.

The case of Fig. 16.8b associated with \mathcal{O}_B in \mathcal{L}_{eff} is new and has no direct relation with semileptonic decays; it belongs to class II. From (61) and (65), we have

$$\begin{aligned} \mathcal{L}_{\text{eff}} &= \frac{G_F}{\sqrt{2}} V_{cb} V_{ud}^* \left\{ \left(c_B + \frac{1}{N_c} c_A \right) \mathcal{O}_B + 2c_A \sum_j [\bar{d} T^j b][\bar{c} T^j u] \right\} \\ &= \frac{G_F}{\sqrt{2}} V_{cb} V_{ud}^* [a_2 \mathcal{O}_B + \dots] , \quad \text{where } a_2 = c_B + \frac{1}{N_c} c_A . \end{aligned} \quad (16.96)$$

The class II is also called color-suppressed decay, since $c_B < c_A$ and in a_2 the dominant coefficient c_A is suppressed by the factor $1/N_c$. All decay modes $\bar{B}^0 \rightarrow H_c^0 + h^0$, where H_c^0 denotes neutral charmed mesons (D^0 , D^{*0} , etc.) and h^0 neutral unflavored mesons (π^0 , ρ^0 , $a_1^0(1260)$, etc.), belong to class II. Also the mode $B \rightarrow J/\psi + K$ is color-suppressed (Fig. 16.9).

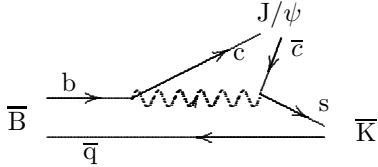


Fig. 16.9. Color-suppressed decay $\bar{B} \rightarrow J/\psi + \bar{K}$

Finally, both $a_1 \mathcal{O}_A$ and $a_2 \mathcal{O}_B$ contribute to the decays $B^- \rightarrow H_c^0 + h^-$ which belong to classe III and illustrated by Fig. 16.10.

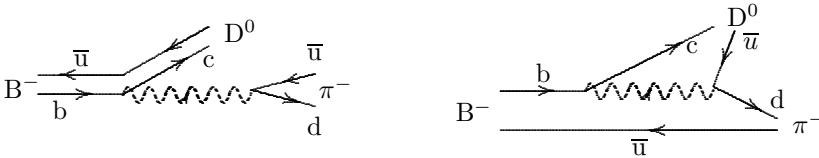


Fig. 16.10. Class III decay: $B^- \rightarrow D^0 + \pi^-$

The decay width $\Gamma(\bar{B}^0 \rightarrow D^+ + \pi^-)$ is directly obtained using the two-body phase space integral given in the Appendix together with (95):

$$\begin{aligned}\Gamma(\bar{B}^0 \rightarrow D^+ + \pi^-) &= \frac{1}{2M_B} \frac{1}{(2\pi)^2} \int \frac{d^3p'}{2E'} \frac{d^3q}{2E_\pi} |\mathcal{M}_{\pi^- D^+}|^2 \delta^4(p - p' - q) \\ &= \frac{a_1^2 G_F^2 |V_{cb} V_{ud}^*|^2}{32\pi} M_B^3 f_\pi^2 \left(1 - \frac{M_D^2}{M_B^2}\right)^3 |f_+(0)|^2. \quad (16.97)\end{aligned}$$

In (97), the pion mass is neglected. As in (93), the amplitude for the decay $\bar{B}^0(p) \rightarrow D^+(p') + \rho^-(q)$ is obtained straightforwardly. Using (13.45) for the ρ^- decay constant $f_{\rho^-} = \sqrt{2} f_{\rho^0} \approx \sqrt{2} \times 150 \text{ MeV}$, one has

$$\begin{aligned}\mathcal{M}_{\rho^- D^+} &= a_1 \frac{G_F}{\sqrt{2}} V_{cb} V_{ud}^* m_\rho f_{\rho^-} [(p + p') \cdot \epsilon_\rho] f_+(m_\rho^2), \\ \Gamma(\bar{B}^0 \rightarrow D^+ + \rho^-) &= \frac{a_1^2 G_F^2 |V_{cb} V_{ud}^*|^2 f_{\rho^-}^2}{32\pi M_B^3} [\lambda(M_B^2, M_D^2, m_\rho^2)]^{\frac{3}{2}} |f_+(m_\rho^2)|. \quad (16.98)\end{aligned}$$

For $\bar{B}^0 \rightarrow D^{*+} + \pi^-$, we need the $\bar{B}^0 \rightarrow D^{*+}$ transition form factors as defined in (76), and only the $A_0(q^2)$ contributes when (76) is multiplied by the pion four-momentum q_μ in $\langle \pi(q) | \bar{d} \gamma_\mu \gamma_5 u | 0 \rangle = i f_\pi q_\mu$:

$$\begin{aligned}\mathcal{M}_{\pi^- D^{*+}} &= i a_1 \frac{G_F}{\sqrt{2}} V_{cb} V_{ud}^* f_\pi [2M_{D^*}] [q \cdot \epsilon_{D^*}] A_0(m_\pi^2), \\ \Gamma(\bar{B}^0 \rightarrow D^{*+} + \pi^-) &= \frac{a_1^2 G_F^2 |V_{cb} V_{ud}^*|^2}{32\pi} M_B^3 f_\pi^2 \left(1 - \frac{M_{D^*}^2}{M_B^2}\right)^3 |A_0(0)|^2, \quad (16.99)\end{aligned}$$

where again the pion mass is neglected. In the class I decays governed by $a_1 \mathcal{O}_A$, the form factors $f_+(q^2)$, $A_0(q^2)$ correspond to the ‘heavy-to-heavy’ $b \rightarrow c$ transitions. With the heavy flavor symmetry (HFS), they are described by the universal function $\xi(\omega)$ and given in (74) and (81).

For the class II decays with $a_2 \mathcal{O}_B$, the involved form factors correspond to the ‘heavy-to-light’ $b \rightarrow d$ transitions. For instance, the amplitude of $\bar{B}^0(p) \rightarrow D^0(p') + \pi^0(q)$ is

$$\mathcal{M}_{\pi^0 D^0} = a_2 \frac{G_F}{\sqrt{2}} V_{cb} V_{ud}^* \langle D^0(p') | \bar{c} \gamma_\mu \gamma_5 u | 0 \rangle \langle \pi^0(q) | \bar{d} \gamma^\mu b | \bar{B}^0(p) \rangle. \quad (16.100)$$

The first factor $\langle D^0(p') | \bar{c} \gamma_\mu \gamma_5 u | 0 \rangle$ can be related to the decay constant f_D defined by $\langle 0 | \bar{c} \gamma_\mu \gamma_5 d | D^+(p') \rangle = i f_D p'_\mu$, and f_D can be extracted in principle from $D^+ \rightarrow \mu^+ + \nu_\mu$, just as f_π is obtained from $\pi^+ \rightarrow \mu^+ + \nu_\mu$. As for the second factor, it can also be related to $\langle \pi^+ | \bar{u} \gamma^\mu b | \bar{B}^0 \rangle$ by isospin rotation:

$$\begin{aligned}\langle \pi^0(q) | \bar{d} \gamma^\mu b | \bar{B}^0(p) \rangle &= \frac{1}{\sqrt{2}} \langle \pi^+(q) | \bar{u} \gamma^\mu b | \bar{B}^0(p) \rangle \\ &= \frac{1}{\sqrt{2}} \left\{ (p + q)^\mu \tilde{f}_+(p'^2) + (p - q)^\mu \tilde{f}_-(p'^2) \right\}.\end{aligned}$$

And so,

$$\mathcal{M}_{\pi^0 D^0} = i a_2 \frac{G_F}{2} V_{cb} V_{ud}^* f_D \left[(M_B^2 - m_\pi^2) \tilde{f}_+(M_D^2) + M_D^2 \tilde{f}_-(M_D^2) \right],$$

from which the rate $\Gamma(\bar{B}^0 \rightarrow D^0 + \pi^0)$ is easily obtained. The heavy-to-light form factors \tilde{f}_\pm are the same as in the decay $\bar{B}^0 \rightarrow \pi^+ + e^- + \bar{\nu}_e$ represented at the quark level by $b \rightarrow u + e^- + \bar{\nu}_e$ which has its rate suppressed by $|V_{ub}|^2 \ll |V_{cb}|^2$. Unlike the ‘heavy-to-heavy’ case, these ‘heavy-to-light’ form factors cannot take advantage of HFS, its theoretical determination may be uncertain and model dependent. Nevertheless, the normalizations $\tilde{f}_\pm(0)$ and the q^2 dependences of $\tilde{f}_\pm(q^2)$ can be determined by $\bar{B}^0 \rightarrow \pi^+ + \ell^- + \bar{\nu}_\ell$ data, although it is a difficult experimental task.

Tests of Factorization. A glance at Fig. 16.7 and Fig. 16.8a together with the corresponding formulas (86) and (97) or (98) immediately gives us the following relation which constitutes a test of factorization:

$$R_h \equiv \frac{\Gamma(\bar{B}^0 \rightarrow H_c^+ + h^-)}{d\Gamma(\bar{B}^0 \rightarrow H_c^+ + e^- + \bar{\nu}_e)/dq^2|_{q^2=m_h^2}} = 6 \pi^2 |a_1|^2 |V_{ud}|^2 f_h^2 X_h, \quad (16.101)$$

where h^- is an unflavored meson like π^- , ρ^- , $a_1(1260)^-$ with their respective decay constants f_h and their corresponding phase space ratio $X_h = M_B^6 / [\lambda(M_B^2, M_{H_c}^2, m_h^2)]^{3/2} \simeq 1$. From the q^2 distribution of the semileptonic decay $d\Gamma(\bar{B}^0 \rightarrow H_c^+ + e^- + \bar{\nu}_e)/dq^2$ at different values of $q^2 = m_h^2$, the relation (101) can be tested. For many modes, the ratios R_h are found to be in good agreement with data¹¹, thus supporting the factorization.

The method is easily extended to other class I decays, in particular the $\bar{B}^0 \rightarrow D^+ + D_s^-$ and $\bar{B}^0 \rightarrow D^+ + D_s^{*-}$ modes, which are also favored by the CKM matrix elements $V_{cb} V_{cs}^*$. Using factorization, one can extract the decay constants f_{D_s} and $f_{D_s^*}$. The $f_{D_s} \approx 240 \text{ MeV}$ obtained from factorization is in agreement with data coming from $D_s^+ \rightarrow \mu^+ + \nu_\mu$.

The decay constant $f_{D_s^*}$ (like f_{K^*}), which cannot be determined by the leptonic mode (since the weak decays $D_s^{*+} \rightarrow \mu^+ + \nu_\mu$, $K^* \rightarrow \mu^+ + \nu_\mu$ are swamped by the strong decays $D_s^* \rightarrow D_s + \pi$, $K^* \rightarrow K + \pi$), nevertheless can be extracted from $\bar{B}^0 \rightarrow D^+ + D_s^{*-}$. Also, the decay constant of the $a_1(1260)$ meson defined in (13.56) can be determined using

$$\frac{\Gamma(\bar{B}^0 \rightarrow D^+ + a_1^-)}{\Gamma(\bar{B}^0 \rightarrow D^+ + \rho^-)} = \frac{f_{a_1}^2}{f_\rho^2} \left[\frac{\lambda(M_B^2, M_D^2, m_{a_1}^2)}{\lambda(M_B^2, M_D^2, m_\rho^2)} \right]^{3/2} \frac{|f_+(m_{a_1}^2)|^2}{|f_+(m_\rho^2)|^2}.$$

One obtains $f_{a_1} \approx 250 \text{ MeV}$ in agreement with the value derived in Chap. 13 from $\tau \rightarrow \nu_\tau + 3\pi$.

¹¹ Browder, T. E. and Honscheid, K., Prog. Nucl. Part. Phys. **35** (1995) 81; Neubert, M. and Stech, B., CERN preprint -TH 97-99 (1997)

16.5 CP Violation in B Mesons

Since 1964, with the discovery of CP violation in $K_L \rightarrow 2\pi$, no new CP-violating phenomenon has been observed although the standard KM mechanism offers a theoretical framework for this effect and opens to CP violation prospects outside the K system, in particular in the bottom sector. B meson decays address three fundamental questions:

(i) Nature and sources of CP violation. Is the KM phase the only mechanism for CP violation? Is it true that only charged currents violate CP whereas neutral currents are CP-conserving as the standard model tells us? As explained in Chap. 11, while the experimental value of the parameter ϵ in the neutral K meson can be accommodated by the standard model, it does not by itself provide a test for it. On the other hand, the ϵ' parameter is subject to theoretical uncertainties because we are in the low-energy regime of nonperturbative QCD, and experimental data for ϵ' are still inconclusive as to whether or not there exists a direct CP violation as predicted by KM.

(ii) CP asymmetries in B^0 decays provide an alternative method to measure the CKM parameters. This is important since the traditional semileptonic modes used for the determination of V_{ub} cannot take advantage of HFS (the u quark is light) and therefore is subject to theoretical uncertainties. Also, the precise values of the CKM matrix elements, in particular those related to the top quark V_{td}, V_{ts} which cannot be directly measured, can be determined. The unitarity of the 3×3 CKM matrix can then be tested, so that the prospect of new fermionic families arises if unitarity does not hold.

(iii) CP asymmetries in the B sector are sensitive to the possible existence of ‘new physics’ beyond the standard model induced by the quantum loop effects of virtual new particles.

16.5.1 B^0 – \bar{B}^0 Mixing

In Chap. 11, the general formalism for the neutral K mesons mixing has been outlined and the formulas (11.39)–(11.49) can be directly applied also to the systems $B_d^0 \equiv \bar{b}d$ and $B_s^0 \equiv \bar{b}s$. We discuss the case of B_d^0 and omit the subscript d for convenience, so that $B_d^0 = B^0$.

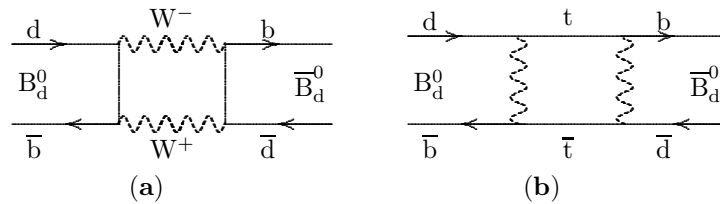


Fig. 16.11a, b. $B_d^0 \leftrightarrow \bar{B}_d^0$ transition through $\bar{b}d \rightarrow \bar{d}b$

Since B^0 can mix with \bar{B}^0 by weak interactions (box diagrams of Fig. 16.11 similar to Fig. 11.1), a neutral B meson weak-interaction eigenstate can be

written as a superposition of B^0 and \bar{B}^0 using a 2×2 mixing matrix $\widetilde{M}_{ij} - \frac{i}{2}\widetilde{\Gamma}_{ij}$ as in (11.41). The off-diagonal terms are responsible for the B^0 – \bar{B}^0 mixing, \widetilde{M}_{12} corresponds to virtual transition between the B^0 and \bar{B}^0 , while $\widetilde{\Gamma}_{12}$ describes real transition due to decay modes which are common to both B^0 and \bar{B}^0 . Similar to (11.43), we introduce a heavy component B_h and a ‘less heavy’ B_l component. They are mixtures of the CP eigenstates, $B_1 = (B^0 - \bar{B}^0)/\sqrt{2}$ and $B_2 = (B^0 + \bar{B}^0)/\sqrt{2}$ of eigenvalues ± 1 respectively:

$$\begin{aligned} B_1 &= p B^0 + q \bar{B}^0 = \frac{1}{\sqrt{1+|\tilde{\epsilon}|^2}} (B_2 + \tilde{\epsilon} B_1) , \\ B_h &= p B^0 - q \bar{B}^0 = \frac{1}{\sqrt{1+|\tilde{\epsilon}|^2}} (B_1 + \tilde{\epsilon} B_2) , \\ \frac{q}{p} &= \frac{1-\tilde{\epsilon}}{1+\tilde{\epsilon}} = \frac{\sqrt{\widetilde{M}_{12}^* - \frac{i}{2}\widetilde{\Gamma}_{12}^*}}{\sqrt{\widetilde{M}_{12} - \frac{i}{2}\widetilde{\Gamma}_{12}}} = \frac{\widetilde{M}_{12}^* - \frac{i}{2}\widetilde{\Gamma}_{12}^*}{\sqrt{\left[\widetilde{M}_{12}^* - \frac{i}{2}\widetilde{\Gamma}_{12}^*\right] \left[\widetilde{M}_{12} - \frac{i}{2}\widetilde{\Gamma}_{12}\right]}} . \end{aligned} \quad (16.102)$$

Indirect CP violation in B^0 – \bar{B}^0 mixing arises if

$$\left| \frac{q}{p} \right| \neq 1 \longrightarrow \tilde{\epsilon} \neq 0 \quad (16.103)$$

which results from the fact that the physical flavor eigenstates B_h and B_l are different from the CP eigenstates B_1 and B_2 .

Let us define $\Delta m_B = M_{B_h} - M_{B_l}$ and $\Delta \Gamma_B = \Gamma_{B_h} - \Gamma_{B_l}$. Similar to (11.45) and (11.46), the diagonalization of the 2×2 matrix $\widetilde{M}_{12} - \frac{i}{2}\widetilde{\Gamma}_{12}$ gives

$$\begin{aligned} M_{B_l} - \frac{i}{2}\Gamma_{B_l} &= M_0 - \frac{i}{2}\Gamma_0 + \sqrt{\left[\widetilde{M}_{12}^* - \frac{i}{2}\widetilde{\Gamma}_{12}^*\right] \left[\widetilde{M}_{12} - \frac{i}{2}\widetilde{\Gamma}_{12}\right]} , \\ M_{B_h} - \frac{i}{2}\Gamma_{B_h} &= M_0 - \frac{i}{2}\Gamma_0 - \sqrt{\left[\widetilde{M}_{12}^* - \frac{i}{2}\widetilde{\Gamma}_{12}^*\right] \left[\widetilde{M}_{12} - \frac{i}{2}\widetilde{\Gamma}_{12}\right]} , \\ \frac{q}{p} &= \frac{-2(M_{12}^* - \frac{i}{2}\Gamma_{12}^*)}{\Delta m_B - \frac{i}{2}\Delta \Gamma_B} = \frac{\Delta m_B - \frac{i}{2}\Delta \Gamma_B}{-2(M_{12} - \frac{i}{2}\Gamma_{12})} , \end{aligned} \quad (16.104)$$

so that

$$\begin{aligned} (\Delta m_B)^2 - \frac{1}{4}(\Delta \Gamma_B)^2 &= 4|\widetilde{M}_{12}|^2 - |\widetilde{\Gamma}_{12}|^2 , \\ (\Delta m_B)(\Delta \Gamma_B) &= 4 \operatorname{Re}(\widetilde{M}_{12}\widetilde{\Gamma}_{12}^*) . \end{aligned} \quad (16.105)$$

The mass difference Δm_B has been measured to be $\approx (0.467 \pm 0.017) (\text{ps})^{-1} = (3.07 \pm 0.11) \times 10^{-4} \text{ eV}$ by the B^0 and \bar{B}^0 oscillations as well as by the

observation of the same sign dilepton events (see below). From (105) we deduce that once Δm_B is known, a tiny $\tilde{\Gamma}_{12} \ll \tilde{M}_{12}$ implies $|\Delta\Gamma_B| \ll \Delta m_B$ and $\Delta m_B \approx 2|\tilde{M}_{12}|$. We first show that $\tilde{\Gamma}_{12} \ll \tilde{M}_{12}$.

For the neutral B^0 and \bar{B}^0 system, the off-diagonal term $\tilde{\Gamma}_{12}$ is extremely small since the overlap in the decay products of B^0 and \bar{B}^0 is rare. Indeed, the B^0 decays mostly into anticharmed and unflavored particles described by $\bar{b} \rightarrow \bar{c} + \bar{d} + u$, while the \bar{B}^0 decays into charm from $b \rightarrow c + d + \bar{u}$. These final decay products are completely distinct. There exist only a few common channels into which both B^0 and \bar{B}^0 decay. They are $B^0 \rightarrow D^+ + D^-$ (or $\pi^+ + \pi^-$) $\leftarrow \bar{B}^0$ coming from $b \rightarrow c + d + \bar{c}$ (or $b \rightarrow u + d + \bar{u}$). However, their rates are suppressed by $|V_{cb}V_{cd}^*|^2$ (or $|V_{ub}V_{ud}^*|^2$). Experimentally, only an upper bound $< 10^{-3}$ is known for the branching ratio into the common decays $B^0 \rightarrow X_{\text{com}}$ and $\bar{B}^0 \rightarrow X_{\text{com}}$.

Therefore, the lifetime difference $\Delta\Gamma_B$ between B_h and B_l is tiny and almost impossible to measure. Neither the long nor the short neutral B mesons are experimentally accessible; however, a mass difference Δm_B exists between the two neutral weak-interaction eigenstates B_h and B_l , which have almost equal lifetimes $\tau_{B^0} = 1/\Gamma_B \approx (1.549 \pm 0.020) \times 10^{-12}$ s.

This is in sharp contrast to the neutral K meson system where the off-diagonal Γ_{12} is large since both K^0 and \bar{K}^0 can decay into the common 2π and 3π channels. With a large Γ_{12} , the K_L and K_S have a large lifetime difference, and therefore they are called K-long and K-short. This unique situation is due to the particular mass scale of the K mesons which have only two hadronic decay modes into 2π and 3π , as discussed in Chap. 11. Both $\Delta m_K = m_L - m_S$ and $\Delta\gamma = \Gamma_S - \Gamma_L$ are comparable, as given in (11.52).

The Ratio $(q/p)_B$ in the B System. For the K system, we know that $2\text{Re}(\bar{\epsilon}) \approx (3.27 \pm 0.12) \times 10^{-3}$ as measured by the electron-positron asymmetry $\delta_K(t)$ in (11.55). Therefore, the ratio $(q/p)_K$ defined in (11.44) for the K system is

$$\left| \frac{q}{p} \right|_K \approx 1 - 2\text{Re}(\bar{\epsilon}) \approx 1 - \mathcal{O}(10^{-3}),$$

a small deviation from 1 of the ratio $|(q/p)_K|$ for the K system is due to CP violation in the $\Delta S = 2$ transition through the K^0 - \bar{K}^0 mixing.

For the B system, on the other hand, independently of the question of CP violation, we can already anticipate from the fact $\tilde{\Gamma}_{12} \ll \tilde{M}_{12}$, i.e. $\tilde{\epsilon} \ll 1$ that the ratio $(q/p)_B$ must be very close to 1. Indeed,

$$\begin{aligned} \left(\frac{q}{p} \right)_B &= \frac{\sqrt{\tilde{M}_{12}^* - \frac{i}{2}\tilde{\Gamma}_{12}^*}}{\sqrt{\tilde{M}_{12} - \frac{i}{2}\tilde{\Gamma}_{12}}} \approx \frac{-\tilde{M}_{12}^*}{|\tilde{M}_{12}|} \left(1 - \frac{1}{2}\text{Im} \left[\frac{\tilde{\Gamma}_{12}}{\tilde{M}_{12}} \right] \right), \\ \left| \frac{q}{p} \right|_B &\approx 1 - \mathcal{O}(10^{-3}). \end{aligned} \quad (16.106)$$

Therefore, indirect CP violation in the $\Delta B = 2$ transition through $B^0-\bar{B}^0$ mixing must be a very small effect, as in the K system. The $\tilde{\epsilon}$ of the B mesons is presumably even smaller than the $\tilde{\epsilon}$ of the K mesons. However, as we will see, direct CP violation in the $\Delta B = 1$ transitions, i.e. in B decays, is expected to be large according to the standard model. This is again in sharp contrast with the K meson in which the $\Delta S = 1$ direct CP violation is vanishingly small [recall the parameter $\epsilon' \ll \epsilon$ (Chap. 11)].

The Mass Difference Δm_B . Once the neutral B mesons are produced in pairs, their semileptonic decays (inclusive or exclusive) provide an excellent method to measure the $B^0-\bar{B}^0$ mixing. From their respective quark contents, B^0 decays into a positive charged lepton ℓ^+ while \bar{B}^0 goes into a negative ℓ^- . If B^0 and \bar{B}^0 do not mix, the produced pair $B^0+\bar{B}^0$ would have a distinctive signature of a dilepton with opposite signs $\ell^+ + \ell^-$. Therefore, a fully reconstructed $\mu^+ + \mu^+$ same-sign event would unambiguously demonstrate the conversion of a \bar{B}^0 into a B^0 , i.e. the pair $B^0-\bar{B}^0$ becomes two B^0 which subsequently decay into $\mu^+ + \mu^+$. This event indeed was found¹² and shows that mixing must exist. Since then, the $B^0-\bar{B}^0$ mixing has a much better statistics¹³

The mass difference Δm_B is a measure of the frequency of the change from a B^0 into a \bar{B}^0 or vice versa. This change is reflected in either the time-dependent oscillations (similar to Fig. 11.2 for the K mesons) or in the time-integrated rates corresponding to the dilepton events having the same sign (see (112) below). Similar to the K_L and K_S system in (11.8), let us write

$$\begin{aligned} |B_h(t)\rangle &= \left[e^{-t\Gamma_B/2} \right] \left(e^{-i t M_B} \right) e^{-i t \Delta m_B/2} |B_h(0)\rangle , \\ |B_l(t)\rangle &= \left[e^{-t\Gamma_B/2} \right] \left(e^{-i t M_B} \right) e^{+i t \Delta m_B/2} |B_l(0)\rangle . \end{aligned} \quad (16.107)$$

The evolution (107) of the mass eigenstates $B_h(t)$ and $B_l(t)$ when combined with (102) gives the time evolution of $B^0(t)$ and $\bar{B}^0(t)$:

$$\begin{aligned} |B^0(t)\rangle &= h_+(t) |B^0(0)\rangle + \frac{q}{p} h_-(t) |\bar{B}^0(0)\rangle , \\ |\bar{B}^0(t)\rangle &= \frac{p}{q} h_-(t) |B^0(0)\rangle + h_+(t) |\bar{B}^0(0)\rangle , \end{aligned} \quad (16.108)$$

$$\begin{aligned} h_+(t) &= e^{-t\Gamma_B/2} e^{-i t M_B} \cos(t \Delta m_B/2) , \\ h_-(t) &= i \left[e^{-t\Gamma_B/2} e^{-i t M_B} \sin(t \Delta m_B/2) \right] . \end{aligned} \quad (16.109)$$

¹² Albrecht, H. et al., Phys. Lett. **192B** (1987) 245

¹³ Wu Sau Lan, in *Proc. 17th Int. Symp. on Lepton-Photon Interactions*, (1995) Beijing (ed. Zheng Zhi-Peng and Chen He-Sheng). World Scientific, Singapore 1996

As in (11.10) and (11.11), starting at $t = 0$ with an initially pure B^0 , the probability for finding a B^0 (\bar{B}^0) at time $t \neq 0$ is given by $|h_+(t)|^2$ ($|h_-(t)|^2$). Taking $|q/p| = 1$, one gets

$$|h_{\pm}(t)|^2 = \frac{1}{2} e^{-t\Gamma_B} [1 \pm \cos(t\Delta m_B)] . \quad (16.110)$$

Conversely, from an initially pure \bar{B}^0 at $t = 0$, the probability for finding a \bar{B}^0 (B^0) at time $t \neq 0$ is also given by $|h_+(t)|^2$ ($|h_-(t)|^2$). The oscillations of B^0 or \bar{B}^0 as shown by (110) give Δm_B directly. Integrating $|h_{\pm}(t)|^2$ from $t = 0$ to $t = \infty$, we get

$$\int_0^\infty dt |h_{\pm}(t)|^2 = \frac{1}{2} \left[\frac{1}{\Gamma_B} \pm \frac{\Gamma_B}{\Gamma_B^2 + (\Delta m_B)^2} \right] . \quad (16.111)$$

The ratio

$$r = \frac{B^0 \leftrightarrow \bar{B}^0}{B^0 \leftrightarrow B^0} = \frac{\int_0^\infty dt |h_-(t)|^2}{\int_0^\infty dt |h_+(t)|^2} = \frac{x^2}{2 + x^2} , \quad \text{where } x \equiv \frac{\Delta m_B}{\Gamma_B} , \quad (16.112)$$

reflects the change of a pure B^0 into a \bar{B}^0 , or vice versa. This change is manifested by the same-sign dilepton events compared to the opposite sign dilepton and yields

$$x = \frac{\Delta m_B}{\Gamma_B} = 0.71 \pm 0.04 . \quad (16.113)$$

This result, when combined with the oscillation measurement, gives the average $\Delta m_B = (3.07 \pm 0.12) \times 10^{-4}$ eV, which is a hundred times larger than the corresponding Δm_K of the K meson system.

The CKM Matrix Element V_{td} from Δm_B . Similar to the Δm_K in Chap. 11, the mass difference Δm_B is calculated from the box diagrams of Fig. 16.11 which give \widetilde{M}_{12} . Contrary to the K meson case where both the charm and the top quark contributions are important, we find that when we apply the formulas (11.36) and (11.37) to the B meson case, the top quark largely dominates \widetilde{M}_{12} . Since $\widetilde{\Gamma}_{12} \ll \widetilde{M}_{12}$ from (105), one has $\Delta m_B \approx 2|\widetilde{M}_{12}|$:

$$\Delta m_B \approx 2|\widetilde{M}_{12}| = \frac{G_F^2 m_t^2 M_B f_B^2}{6\pi^2} g(x_t) \eta_t |V_{td}^* V_{tb}|^2 B , \quad (16.114)$$

where $\eta_t \approx 0.55$ is the gluonic correction¹⁴ to the box diagrams, $g(x_t)$ is already given in (11.37), f_B is the B meson decay constant involved in $B^+ \rightarrow \tau^+ + \nu_\tau$ similar to the decay constants f_π, f_K, f_D . The last factor B , like

¹⁴ Buras, A., Jamin, M. and Weizs, P. H., Nucl. Phys. **B347** (1990) 491

the one defined in (11.29), represents the correction to the vacuum insertion used in the evaluation of Δm_B . The decay constant f_B , not yet determined by experiments, is taken to be 180 ± 50 MeV and the parameter B is taken as 1 ± 0.2 , both values obtained from lattice calculations¹⁵. Then (114) gives

$$|V_{td}| = (9.2 \pm 3) \times 10^{-3} = A \lambda^3 \sqrt{(1 - \rho)^2 + \eta^2} \quad (16.115)$$

which represents one more constraint on the parameters ρ and η of the CKM matrix, in addition to (60):

$$|1 - \rho - i\eta| = 1.01 \pm 0.22$$

From (112) and (114), we realize that the $B^0 - \bar{B}^0$ mixing can be observed because of the large Δm_B or, equivalently, because of the large top quark mass which compensates for the small $|V_{td}^*|^2$.

Using (106) and (114), one finds the following expression frequently used:

$$\left(\frac{q}{p}\right)_B = \frac{\sqrt{\widetilde{M}_{12}^* - \frac{i}{2}\widetilde{\Gamma}_{12}^*}}{\sqrt{\widetilde{M}_{12} - \frac{i}{2}\widetilde{\Gamma}_{12}}} \approx \frac{\sqrt{\widetilde{M}_{12}^*}}{\sqrt{\widetilde{M}_{12}}} = \frac{\sqrt{(V_{td}V_{tb}^*)^2}}{\sqrt{(V_{td}^*V_{tb})^2}} = \frac{V_{td}V_{tb}^*}{V_{td}^*V_{tb}} \equiv e^{-2i\beta}, \quad (16.116)$$

which tells us that to a very good approximation the ratio q/p is a pure phase. The angle β which characterizes the standard CP violating mechanism is an important quantity in the unitarity triangle we are considering now.

Unitarity Triangles. As discussed in (11.85), the unitarity of the CKM matrix is visualized by six triangles, all of which have the same area $\frac{1}{2}J$, and the standard CP violating mechanism is reflected by $J \neq 0$. In a phase reparameterization of the quark fields that build the CKM matrix, the triangles change their orientation in the plane, but their shape remains unaffected. Among the six triangles, only two have a regular shape due to the fact that their three sides are not dissimilar and proportional to λ^3 where $\lambda = \sin \theta_C \approx 0.22$. The remaining four triangles always have one side much smaller than the other two sides. These two regular triangles are those which connect the CKM matrix elements that belong either to the first and the third columns, or to the first and the third rows. The triangle illustrated in Fig. 16.12 comes from

$$V_{ud}V_{ub}^* + V_{cd}V_{cb}^* + V_{td}V_{tb}^* = 0. \quad (16.117)$$

Figure 16.12b is taken from Fig. 16.12a by dividing all sides by $V_{cd}V_{cb}^*$. This quantity by convention is taken to be real. The rescaled triangle has the coordinates $(0,0)$, $(1,0)$ and $(\bar{\rho},\bar{\eta})$ with $\bar{\rho} = \rho(1 - \frac{1}{2}\lambda^2)$, $\bar{\eta} = \eta(1 - \frac{1}{2}\lambda^2)$. Physical quantities measuring CP violation can be expressed in terms of J or, equivalently, of the angles α, β, γ . Now we show that these angles can be obtained by measuring the differences between the B and \bar{B} decay rates into various channels due to CP violation.

¹⁵ Michael, C., in *Proc. 17th Int. Symp. on Lepton-Photon Interactions*, (1995) Beijing (ed. Zheng Zhi-Peng and Chen He-Sheng). World Scientific, Singapore 1996

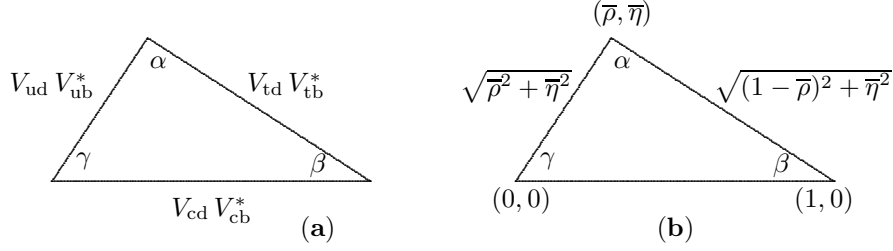


Fig. 16.12a,b. The angles α, β, γ of the unitarity triangle

16.5.2 CP Asymmetries in Neutral B Meson Decays

The most promising method of measuring CP violation is to look for an asymmetry between the $\Gamma(B^0 \rightarrow f_{\text{cp}})$ and $\Gamma(\bar{B}^0 \rightarrow \bar{f}_{\text{cp}})$, where f_{cp} is a hadronic state having a well-defined CP eigenvalue ± 1 . These states of definite CP parities are called CP eigenstates. We have $\bar{f}_{\text{cp}} = \pm f_{\text{cp}}$ depending on the CP parity of f_{cp} . Some examples of CP eigenstates are the two-particle systems: $\psi + K_S$ (CP parity = -1), $\pi^+ + \pi^-$ (CP parity = +1), and $\rho^0 + K_S$ (CP parity = -1). Next, we define the amplitudes A , \bar{A} and the parameter ξ as

$$A \equiv \langle f_{\text{cp}} | H_W | B^0 \rangle, \quad \bar{A} \equiv \langle \bar{f}_{\text{cp}} | H_W | \bar{B}^0 \rangle, \quad \xi \equiv \frac{q}{p} \frac{\bar{A}}{A}. \quad (16.118)$$

The time evolution of the decay amplitudes can be written as

$$\begin{aligned} \langle f_{\text{cp}} | H_W | B^0(t) \rangle &= A [h_+(t) + \xi h_-(t)], \\ \langle \bar{f}_{\text{cp}} | H_W | \bar{B}^0(t) \rangle &= \frac{p}{q} A [h_-(t) + \xi h_+(t)]. \end{aligned} \quad (16.119)$$

The rates for an initial pure B^0 (or \bar{B}^0) to decay into a CP eigenstate f_{cp} (or \bar{f}_{cp}) at time t are given by

$$\begin{aligned} \Gamma(B^0(t) \rightarrow f_{\text{cp}}) &= C \left[\frac{1 + |\xi|^2}{2} + \frac{1 - |\xi|^2}{2} \cos(\Delta m_B t) - \text{Im}(\xi) \sin(\Delta m_B t) \right], \\ \Gamma(\bar{B}^0(t) \rightarrow \bar{f}_{\text{cp}}) &= C \left[\frac{1 + |\xi|^2}{2} - \frac{1 - |\xi|^2}{2} \cos(\Delta m_B t) + \text{Im}(\xi) \sin(\Delta m_B t) \right] \end{aligned}$$

where $C = |A|^2 e^{-\Gamma_B t}$. The time-dependent CP asymmetry is defined as

$$\begin{aligned} a(t) &= \frac{\Gamma(B^0(t) \rightarrow f_{\text{cp}}) - \Gamma(\bar{B}^0(t) \rightarrow \bar{f}_{\text{cp}})}{\Gamma(B^0(t) \rightarrow f_{\text{cp}}) + \Gamma(\bar{B}^0(t) \rightarrow \bar{f}_{\text{cp}})} \\ &= \frac{(1 - |\xi|^2) \cos(\Delta m_B t) - 2 \text{Im}(\xi) \sin(\Delta m_B t)}{1 + |\xi|^2}. \end{aligned} \quad (16.120)$$

We have seen in (116) that $|q/p| = 1$. Furthermore, if $|\bar{A}/A| = 1$ so that $|\xi| = 1$, the asymmetry $a(t)$ simplifies considerably:

$$a(t) = -\text{Im}(\xi) \sin(\Delta m_B t) . \quad (16.121)$$

The total rate asymmetry is obtained by integrating the numerator and denominator of (120). For $|\xi| = 1$, we have

$$\bar{a} = \frac{\int_0^\infty dt \left\{ \Gamma(B^0(t) \rightarrow f_{\text{cp}}) - \Gamma(\bar{B}^0(t) \rightarrow \bar{f}_{\text{cp}}) \right\}}{\int_0^\infty dt \left\{ \Gamma(B^0(t) \rightarrow f_{\text{cp}}) + \Gamma(\bar{B}^0(t) \rightarrow \bar{f}_{\text{cp}}) \right\}} = \frac{-x}{1+x^2} \text{Im}(\xi) , \quad (16.122)$$

where x is given in (113). We note that the integrated asymmetry \bar{a} is suppressed when $x \ll 1$ (case of charmed D^0 mesons, since $\Gamma_D \gg \Delta m_D$) or when $x \gg 1$ (case of $B_s^0 \equiv \bar{b}s$). In these cases, the time-dependent asymmetry $a(t)$ is appropriately useful.

When $|\xi| = 1$, the quantity ξ , which may be written as $\xi = e^{i\theta}$, is very interesting since its imaginary part, i.e. $\sin \theta$, is directly related to the CKM matrix elements, such that measurements of the asymmetries directly determine the CKM angles. So our next task is to look for the conditions that guarantee $|\bar{A}/A| = 1$.

As already illustrated by (11.64) and (11.65) for $K^0 \rightarrow 2\pi$ and $\bar{K}^0 \rightarrow 2\pi$ processes, in general the amplitudes of B^0 and \bar{B}^0 decaying into an arbitrary state can be written as the sum of various contributions,

$$A = \sum_k A_k e^{i\delta_k} e^{i\phi_k} , \quad \bar{A} = \sum_k A_k e^{i\delta_k} e^{-i\phi_k} , \quad (16.123)$$

where ϕ_k is the weak interaction CKM phase that represents CP violation while δ_k is the strong-interaction phase-shift due to rescattering effects among the hadrons in the final state. The δ_k enters A and \bar{A} without changing sign since the strong interactions conserve CP. Thus $|A| = |\bar{A}|$ if the various contributions A_k have the same CKM phase, or in particular, if there is only one dominant contribution. In these special cases, the hadronic uncertainties essentially due to the unknown δ_k are eliminated in the ratio $|\bar{A}/A| = 1$. But generally $|\bar{A}/A| \neq 1$, since nonleptonic decays in (123) receive contributions from both the ‘tree’ and ‘penguin’ amplitudes. The former – if favored by the CKM matrix elements (say $V_{cb}V_{ud}^*$ or $V_{cb}V_{cs}^*$) – would dominate the latter which are suppressed by QCD perturbative higher orders. However, it is not difficult to find some counterexamples where ‘tree’ amplitudes are either forbidden or suppressed by $V_{ub}V_{us}^* \sim 10^{-3} V_{cb}V_{ud}^*$. Furthermore, tree and penguin amplitudes have different CKM phases in general.

Fortunately, there exist a few cases where $|\bar{A}/A| = 1$. In particular, we are interested in $b \rightarrow s + c + \bar{c}$ (responsible for the decay mode $B \rightarrow J/\psi + K$) which in turn allows the determination of the angle β . This mode receives

contributions from both tree and penguin diagrams. However, we will see that $|\bar{A}/A| = 1$ still holds.

Generically, the penguin diagram is always of the type $b \rightarrow s (d) + q + \bar{q}$ and shown in Fig. 16.13a. We note that the internal loop is dominated by the top quark because of its mass and also because $V_{tb} \approx 1$ is largest. The dominant penguin amplitude corresponds to the process $b \rightarrow s + q + \bar{q}$ (for instance $b \rightarrow s + c + \bar{c}$ or $b \rightarrow s + u + \bar{u}$). The amplitude can be directly taken from $H_{\text{pen}}^{\text{glu}}$ given in (11.94). Let us write it as

$$\frac{\alpha_s}{12\pi} V_{tb} V_{ts}^* \log \frac{m_t^2}{m_b^2}, \quad (16.124)$$

where the factor $G_F/\sqrt{2}$, the quark fields, and the Dirac matrices explicitly written in (11.94) are omitted here for simplicity. The nondominant penguin diagram $b \rightarrow d + q + \bar{q}$ can be taken from (124) by replacing V_{ts}^* with $V_{td}^* < V_{ts}^*$.

The same $b \rightarrow s + c + \bar{c}$ amplitude due to the tree diagram (Fig. 16.13b) is proportional to $V_{cb} V_{cs}^*$, which is larger than (124).

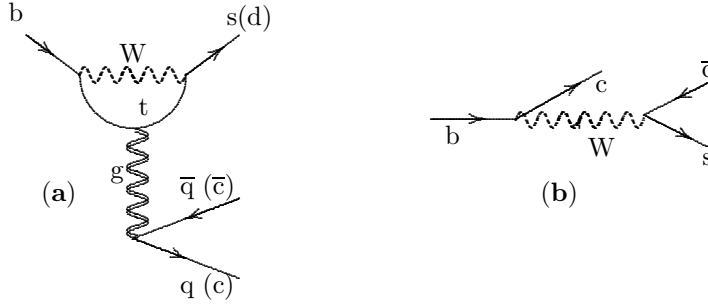


Fig. 16.13. The transition $b \rightarrow s + c + \bar{c}$ by (a) penguin (b) tree diagram

Within the standard KM mechanism of CP violation, the decay mode $\bar{B} \rightarrow J/\psi + K_S$ is very interesting since, not only the tree amplitude dominates the penguin amplitude, but both amplitudes have a common CKM phase such that independently of their relative magnitude, the condition $|A| = |\bar{A}|$ is fulfilled. Adding the penguin part to the tree diagram amplitude in (123) does not affect $|\xi| = 1$, so that the asymmetry in (121) or (122) is theoretically very clean. For this reason, the asymmetry of this ‘gold-plated’ mode would be the first to be measured in the future B meson factories. This decay has already been observed with a branching ratio $\sim 10^{-3}$. So the next experimental task is to measure the asymmetry, which needs a much larger statistics.

The decay $\bar{B} \rightarrow J/\psi + K_S$ issued from $\bar{B} \rightarrow J/\psi + \bar{K}$ is governed at the quark level by $b \rightarrow c + s + \bar{c}$ for which the amplitude of the tree diagram is proportional to $V_{cb} V_{cs}^*$ as mentioned previously. The other details of the amplitude are irrelevant. The transition of \bar{K} into K_S will be discussed later.

The penguin amplitude for the same reaction $\bar{B} \rightarrow J/\psi + \bar{K}$, as shown by (124), has the $V_{tb}V_{ts}^*$ factor. This factor has the same phase as the tree amplitude $V_{cb}V_{cs}^*$, so even with the sum of the tree and penguin amplitudes in (123), we still have $|\bar{A}/A| = 1$ since

$$\frac{\bar{A}}{A} = \frac{V_{cb}V_{cs}^*}{V_{cb}^*V_{cs}}. \quad (16.125)$$

Let us emphasize that, independently of the details of both the tree (Fig. 16.9) and penguin (Fig. 16.14) decay amplitudes, the ratio \bar{A}/A is model independent and always given by (125). This ratio is sufficient for a prediction of the asymmetry.

There remains the factor q/p for ξ in (118). In fact, there are two q/p . One, associated with the B system $(q/p)_B$, is already known in (116) and the other, $(q/p)_K$, is still to be determined since, with a K_S in the final state, one has to take into account the mixing of K^0 and \bar{K}^0 in the K_S too. For this purpose, we must look for the ratio

$$\left(\frac{q}{p}\right)_K \equiv \frac{\langle K_S | \bar{K} \rangle}{\langle K_S | K \rangle}.$$

We write $K_S = p_K K^0 + q_K \bar{K}^0$, then $\langle K_S | \bar{K} \rangle = q_K^*$, $\langle K_S | K \rangle = p_K^*$, so

$$\left(\frac{q}{p}\right)_K = \frac{q_K^*}{p_K^*}.$$

The ratio q_K/p_K comes from M_{12} in (11.80) of the box diagram in Fig. 11.1. This ratio q_K/p_K can be directly taken from q_B/p_B with the substitution $b \leftrightarrow s$ and $t \leftrightarrow c$ which is suggested by comparing the box diagrams in Fig. 11.1 and Fig. 16.11. Thus

$$\left(\frac{q}{p}\right)_K = \left(\frac{V_{cs}^*V_{cd}}{V_{cs}V_{cd}^*}\right)^* = \frac{V_{cs}V_{cd}^*}{V_{cs}^*V_{cd}}. \quad (16.126)$$

Using (116), (125), and (126), the parameter ξ in (118) for $B \rightarrow J/\psi + K_S$ is

$$\begin{aligned} \xi_{\psi K_S} &= \left(\frac{q}{p}\right)_B \left(\frac{q}{p}\right)_K \frac{V_{cb}V_{cs}^*}{V_{cb}^*V_{cs}} = \left(\frac{V_{td}V_{tb}^*}{V_{td}^*V_{tb}}\right) \left(\frac{V_{cs}V_{cd}^*}{V_{cs}^*V_{cd}}\right) \left(\frac{V_{cb}V_{cs}^*}{V_{cb}^*V_{cs}}\right) \\ &= \left(\frac{V_{td}V_{tb}^*}{V_{td}^*V_{tb}}\right) \left(\frac{V_{cd}^*V_{cb}}{V_{cd}V_{cb}^*}\right) = \left(\frac{V_{td}V_{tb}^*}{V_{td}^*V_{tb}}\right) = e^{-2i\beta} \end{aligned}$$

since $V_{cd}V_{cb}^*$ is real (see Fig. 16.12). Note that the CP eigenstate $J/\psi + K_S$ has intrinsic CP parity -1 ; the ratio \bar{A}/A has an extra minus sign so that actually $\xi_{\psi K_S} = -\exp(-2i\beta)$, and consequently the asymmetries $a(t)$ and \bar{a} defined in (121) and (122) are proportional to $-\sin(2\beta)$.

Therefore, a measurement of the asymmetry in $B \rightarrow J/\psi + K_S$ directly gives the β angle. From our present knowledge of the values of the CKM parameters ρ and η as given by (60), (115) and depicted in Fig. 16.12, one may take $0.3 \leq \sin 2\beta \leq 0.8$, such that the asymmetry \bar{a} is expected to be in the range $-0.4 \leq \bar{a} \leq -0.15$ with a *negative sign*.

We finally mention that asymmetries are also expected in many other modes, such as for instance in charged B^\pm meson decays. The condition

$$\left| \frac{\bar{\mathcal{A}}}{\mathcal{A}} \right| \neq 1 \quad (16.127)$$

implies direct CP violation, where $\mathcal{A} = \langle \mathcal{F} | H_W | B^+ \rangle$ and $\bar{\mathcal{A}} = \langle \bar{\mathcal{F}} | H_W | B^- \rangle$. Note that contrary to the case where $\mathcal{F} = f_{\text{CP}}$ which gives $|\bar{\mathcal{A}}/\mathcal{A}| = 1$ in (118), since the final state \mathcal{F} is not a CP eigenstate, the condition (127) requires at least two partial amplitudes A_k in (123) that differ in both their weak and strong interaction ϕ_k and δ_k phases.

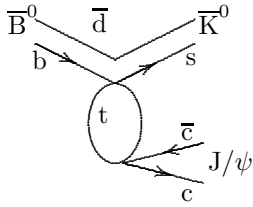


Fig. 16.14. $\bar{B} \rightarrow \bar{K} + J/\psi$ by penguin transition

The standard CP-violating KM mechanism is very predictive since all CP violation phenomena are described by a single parameter which can be taken as J . The interesting asymmetry in $B \rightarrow J/\psi + K_S$, which is free of hadronic uncertainties in the evaluation of the decay amplitude, is the best example; it can be used as a consistency check of the KM mechanism. Therefore, once the various CP asymmetries in B mesons are measured, deviations from these predictions, if they arise, would provide clues about the new physics beyond the standard model.

Problems

16.1 The $|\Delta I| = \frac{1}{2}$ rule and the penguin operator. Show that the matrix element of the penguin operator $\mathcal{O}_{\text{pen}} = [\bar{d} \gamma_\mu (1 - \gamma_5) \lambda^b s] [\bar{q} \gamma^\mu \lambda^b q]$ in (11.94) inserted between the K and $\pi\pi$ states can be enhanced by terms proportional to $1/m_q$ where q are light u, d, or s quarks. So they contribute to the $|\Delta I| = \frac{1}{2}$ rule in the right direction.

16.2 The decay constant f_B . To extract the decay constant f_B , what are the relevant decay modes of the B meson to look for? Estimate the corresponding branching ratios.

16.3 The rare decay $B \rightarrow \gamma + K^*$. At the quark level, show that this mode is governed by $b \rightarrow \gamma + s$. Draw the corresponding Feynman diagram and estimate the amplitude using the calculation outlined in Chap. 11 for gluonic penguin. Explain why the mode $B \rightarrow \gamma + K$ is forbidden (more generally, any transition of the pseudoscalar mesons $0^- \rightarrow 0^- + \gamma$ vanishes). The rare modes are interesting due to possible effects of new particles in the loops.

16.4 Relations among $B \rightarrow K(K^*)$ and $D \rightarrow K(K^*)$ form factors. These form factors are of the type ‘heavy-to-light’ transitions, hence heavy flavor symmetry cannot be applied. However, using HFS, one may derive

$$\frac{\langle K(p') | V_\mu | B(v) \rangle}{\sqrt{M_B}} = \frac{\langle K(p') | V_\mu | D(v) \rangle}{\sqrt{M_D}}$$

up to corrections $\mathcal{O}(1/M)$. Since the form factors are evaluated with the *velocity* transfer $(v - v')^2$, show that

$$f_{\pm}^{B \rightarrow K}(t_B) = \left[\frac{M_B + M_D}{2\sqrt{M_B M_D}} f_{\pm}^{D \rightarrow K}(t_D) - \frac{M_B - M_D}{2\sqrt{M_B M_D}} f_{\mp}^{D \rightarrow K}(t_D) \right], \quad (16.128)$$

where t_B and t_D are related by

$$v_B \cdot v_K = v_D \cdot v_K \implies M_D t_B - M_B t_D = [M_B - M_D][M_B M_D - M_K^2]. \quad (16.129)$$

The interest of these relations lies in the fact that the $D \rightarrow K(K^*)$ form factors can be determined by experiments on semileptonic D decays; whereas the $B \rightarrow K(K^*)$ form factors are not accessible by semileptonic modes. By factorization, the $B \rightarrow K(K^*)$ form factors are involved in nonleptonic color-suppressed decays. Compute the $B \rightarrow J/\psi + K$ rate in terms of the $D \rightarrow K$ form factors.

16.5 Inclusive B meson semileptonic branching ratio. Compute the branching ratio B_{sl} , using the formulas (57), (67), and (68)

$$B_{sl} \equiv \frac{\Gamma(B \rightarrow X_c + e^- + \bar{\nu}_e)}{\Gamma_{tot}}.$$

16.6 The CKM angles α and γ . Show that the CP asymmetry between $B^0 \rightarrow \pi^+ + \pi^-$ and $\bar{B}^0 \rightarrow \pi^+ + \pi^-$ gives the α angle. The angle γ comes from the asymmetry between the $B_s^0 \rightarrow \rho^0 + K_S$ and $\bar{B}_s^0 \rightarrow \rho^0 + K_S$. Show that the tree and penguin amplitudes of these modes do not have the same phase, in contradistinction with the best mode $J/\psi + K_S$.

Suggestions for Further Reading

QCD *corrections to weak interaction, operator product expansion:*

Peskin, M. E. and Schroeder, D. V., *An Introduction to Quantum Field Theory*. Addison-Wesley, Reading, MA 1995

Wilson, K., Phys. Rev **179** (1969) 1499

Heavy flavor symmetry:

Isgur, N. and Wise, M. B., in *B Decays* (ed. Stone, S.). World Scientific, Singapore 1994

CP *violation:*

Bigi, I. I., Khoze, V. A., Uraltsev, N. G. and Sanda, A. I., in *CP violation* (ed. Jarlskog, C.). World Scientific, Singapore 1989

Buras, A. J. and Harlander, M. K., in *Heavy Flavors* (ed. Buras, A. J. and Lindner, M.). World Scientific, Singapore 1992

Nir, Y. and Quinn, H., in *B Decays* (op. cit.)

Rosner, J. L., *Present and Future Aspect of CP Violation*, Proc. of the VIII J. A. Swieca Summer School on Particles and Fields (ed. Barcelos-Neto, J., Novaes, S. F. and Rivelles, V. O.). World Scientific, Singapore 1996